2013

LANL-CO ACRSP
LCO-ACP-14

Jean Francois Lucchini
Michael Richmann
Marian Borkowski

Uranium (VI) Solubility in WIPP Brine

LA-UR 13-20786

Page left intentionally blank

Uranium (VI) Solubility in WIPP Brine

J.F. Lucchini,
M.K. Richmann, and M. Borkowski

EXECUTIVE SUMMARY

The solubility of uranium (VI) in Waste Isolation Pilot Plant (WIPP)-relevant brine was determined as part of an overall effort to establish a more robust WIPP chemistry model to support ongoing WIPP recertification activities. This research was performed as part of the Los Alamos National Laboratory Carlsbad Operations (LANL-CO) Actinide Chemistry and Repository Science Program (ACRSP).

The WIPP Actinide Source Term Program (ASTP) did not develop a model for the solubility of actinides in the VI oxidation state. The upper limit of the solubility of UO_2^{2+}, in the absence of WIPP-specific data, is presently set at 10^{-3} M in the WIPP Performance Assessment (PA) for all expected conditions. This value was selected at the recommendation of the Environment Protection Agency (EPA), based on their review of the relevant data available in the literature and accounts for the potential and likely effects of carbonate complexation on the solubility of uranium (VI).

In this report, the results of experiments to establish the solubility of U(VI) in WIPP brines are presented. The solubility of uranium (VI) was determined in WIPP-relevant brines as a function of pC_{H+}, and in the absence or presence of carbonate. A major objective of these experiments was to provide experimental data on the effects of carbonate complexation on uranium (VI) solubility in WIPP brines. These experiments were performed in compliance with the DOE Carlsbad Field Office, Quality Assurance Program Document (CBFO/QAPD). A literature review on the solubility of U(VI) under WIPP-related conditions was also conducted, and is reported herein.

There are a number of key results and observations from this U(VI) solubility study and the literature search that was performed. The most important of these are:

- There were no WIPP-specific experimental data available in the literature on VI actinide solubility in carbonate-free conditions. The two WIPP-relevant papers found in the literature were from Yamazaki [1992] and Diaz-Arocas [1998]. They determined the solubility of uranium (VI) in conditions close to those expected in WIPP (brine, high ionic strength, basic pH), but with less rigorous control of a carbon dioxide free environment than in our experiments. The values reported by Yamazaki [1992] and Diaz-Arocas [1998] were in the range 10^{-7} – 3×10^{-3} M.

- The solubility data for uranium (VI) in WIPP brine presented in this report accomplished the following:
  - Provided the first WIPP-relevant data for the VI actinide oxidation state that established the solubility of uranium (VI) over an extended pC_{H+} range for GWB and ERDA-6 brines in the absence or presence of carbonate.
  - Established an upper limit of ~ 10^{-6} M uranyl concentration at the reference pC_{H+} WIPP case in the absence of carbonate, and an upper limit of ~ 10^{-4} M uranyl concentration at the reference pC_{H+} WIPP case (i.e., pC_{H+} ~ 9.5) in the presence of 2mM carbonate. These solubilities are 10-100 times lower than published results.
  - Demonstrated that high pC_{H+} values lead to low uranium solubility due to hydrolysis, in carbonate-free and low carbonate content WIPP brines. At $pC_{H+} \geq 10.5$, hydrolysis overwhelms carbonate effects. No amphoteric effect was observed in WIPP simulated brines at high pC_{H+} values.
  - Demonstrated a small effect of borate complexation in the pC_{H+} range [7.5 – 10].
- In the absence of carbonate, the uranium (VI) solubilities measured in our experiments were about 10^{-6} M in GWB brine at $pC_{H+} \geq 7$ and about 10^{-8} - 10^{-7} M in ERDA-6 at $pC_{H+} \geq 8$.
- The observed effects of carbonate on the solubility of U(VI) in WIPP-specific brines are directly relevant to the current PA assumption. For WIPP-related conditions (i.e., pC_{H+} ~ 9.5), the highest uranium solubility obtained experimentally was ~ 10^{-4} M for a carbonate concentration (2×10^{-3} M), which was ~ 10 times higher amount of carbonate expected in the WIPP due to the buffering of the MgO barrier material. In this context, these data provide a direct experimental confirmation of the current PA assumption that the solubility of U(VI) will be 1 mM or less.

The authors wish to thank Russ Patterson (DOE/CBFO) for his support to the LANL-CO/ACRSP. All research was performed at the Carlsbad Environmental and Monitoring Research Center (CEMRC), managed by New Mexico State University (NMSU) and located in Carlsbad, NM. Funding for this research is through the WIPP, managed by DOE/CBFO.

TABLE OF CONTENTS

LIST OF FIGURES AND TABLES

Figures

Tables

LIST AND DEFINITION OF ACRONYMS, ABBREVIATIONS, ELEMENTS AND CHEMICAL COMPOUNDS

ºC	Degrees Celsius
%	Percent
ACRSP	Los Alamos Actinide Chemistry and Repository Science Program
ACS	American Chemical Society
Ar	Argon
Am	Americium
An	Actinide
An(III)	General Actinide in the III oxidation state
An(IV)	General Actinide in the IV oxidation state
An(V)	General Actinide in the V oxidation state
An(VI)	General Actinide in the VI oxidation state
ASTP	WIPP Actinide Source Term Program
Å	Angstrom
β^o	Stability constant at reference state
C_M	Concentration of M species
$CaCl_2$	Calcium chloride
$CaCO_3$	Calcium carbonate
(DOE) CBFO	(Department of Energy) Carlsbad Field Office
CCA	Compliance Certification Application
CEMRC	Carlsbad Environmental Monitoring and Research Center
CO_2	Carbon dioxide
CO_2(aq)	Carbon dioxide gas dissolved in solution
CO_3^{2-}	Carbonate ion
CRA	Compliance Recertification Application
DOE	US Department of Energy
EDS	Energy-Dispersive x-ray Spectrometer
EPA	US Environment Protection Agency
ERDA-6	(U.S.) Energy Research and Development Administration (WIPP well) 6, a synthetic brine representative of fluids in Castile brine reservoirs

EXAFS	Extended X-ray Absorption Fine Structure
Fe	Iron
FMT	Fracture-Matrix Transport model
g	Gram
GWB	Generic Weep Brine, a synthetic brine representative of fluids in Salado brine reservoirs
H^+	Hydrogen ion
HCO_3^-	Bicarbonate ion
H_2O	Water
H_2O_2	Hydrogen peroxide
$H_2CO_3(aq)$	Carbonic acid
HP water	High Purity water, i.e. deionized water with a specific resistance of 18.0 megaohm-cm or greater at room temperature
I	Ionic strength
ICP-MS	Inductively Coupled Plasma-Mass Spectrometry
kDa	kiloDalton
K_{a1}	First dissociation constant for carbonic acid
K_{a2}	Second dissociation constant for carbonic acid
K_h	Hydrolysis constant of carbonic acid
K_W	Dissociation constant of water
KNO_3	Potassium nitrate
$K_2U_2O_7$	Potassium diuranate
KCl	Potassium chloride
L	Liter
LANL	Los Alamos National Laboratory
LANL-CO	Los Alamos National Laboratory - Carlsbad Operations
LiCl	Lithium chloride
mL	Milliliter
mM	Millimole
M	Mole per liter
$MgCl_2$	Magnesium chloride
$Mg(OH)_2$	Brucite, magnesium hydroxide
MΩ·cm	Megaohm-centimeter
$Na_2B_4O_7$	Sodium tetraborate
Na_2CO_3	Sodium carbonate
Na_2SO_4	Sodium sulfate

$Na_2U_2O_7.xH_2O$	Sodium diuranate hydrate
NaBr	Sodium bromide
NaCl	Sodium chloride
NIST	National Institute of Standards and Technology
nm	Nanometer
NMSU	New Mexico State University
N_2	Nitrogen
Np	Neptunium
Np(VI)	Neptunium in the VI oxidation state
O_2	Oxygen
OH^-	Hydroxyl ion
PA	Performance Assessment
PABC	Performance Assessment Baseline Calculation
PAVT	Performance Assessment Verification Test
pC_{H+}	Negative logarithm of H^+ concentration
pH	Negative logarithm of H^+ activity
pH_{obs}	Measured/Observed pH
pKa	Negative logarithm of the dissociation constant of an acid
ppb	Parts per billion
ppm	Parts per million
Pu	Plutonium
Pu(III)	Plutonium in the III oxidation state
Pu(IV)	Plutonium in the IV oxidation state
Pu(VI)	Plutonium in the VI oxidation state
rpm	Revolution per minute
QA	Quality Assurance
QAPD	Quality Assurance Program Document
SEM	Scanning Electron Microscopy
SOTERM	Actinide Source Term appendix for WIPP recertification applications
T	Temperature
Th	Thorium
Th(IV)	Thorium in the IV oxidation state
TRU	Transuranic (actinides higher in atomic number than uranium)
U	Uranium
U(IV)	Uranium in the IV oxidation state

U(VI)	Uranium in the VI oxidation state
UO_2^{2+}	Uranyl ion – Aqueous form of the uranium at the VI oxidation state
UO_2CO_3	Rutherfordine, uranium (VI) carbonate
$UO_2(CO_3)_2^{2-}$	Uranium (VI) carbonate ion – (1:2) complex
$UO_2(CO_3)_3^{4-}$	Uranium (VI) carbonate ion – (1:3) complex or triscarbonato complex
$(UO_2)_3(CO_3)_6^{6-}$	Uranium (VI) carbonate ion – (3:6) complex
$(UO_2)_2(CO_3)(OH)_3^-$	Uranium (VI) carbonate hydroxide ion – (2:1:3) complex
$(UO_2)_{11}(CO_3)_6(OH)_{12}^{2-}$	Uranium (VI) carbonate hydroxide ion – (11:6:12) complex
$UO_2(NO_3)_2 \cdot 6H_2O$	Depleted uranium (VI) nitrate hexahydrate
$UO_2(OH)^+$	Uranium (VI) hydroxide ion – (1:1) complex
$UO_2(OH)_2$	Uranium (VI) hydroxide
$UO_2(OH)_3^-$	Uranium (VI) hydroxide ion – (1:3) complex
$UO_2(OH)_4^{2-}$	Uranium (VI) hydroxide ion – (1:4) complex
$(UO_2)_2OH^{3+}$	Dimer uranium (VI) hydroxide ion – (2:1) complex
$(UO_2)_2(OH)_2^{2+}$	Dimer uranium (VI) hydroxide ion – (2:2) complex
$(UO_2)_2(OH)_2Cl_2(H_2O)_4$	(2:2:2) uranium (VI) hydroxide chloride complex
$[(UO_2)_2(OH)_2(NO_3)_2(H_2O)_3] \bullet H_2O$	(2:2:2) uranium (VI) hydroxide nitrate complex hydrated
$(UO_2)_3(OH)_4^{2+}$	Trimer uranium (VI) hydroxide ion – (3:4) complex
$(UO_2)_3(OH)_5^+$	Trimer uranium (VI) hydroxide ion – (3:5) complex
$(UO_2)_3(OH)_7^-$	Trimer uranium (VI) hydroxide ion – (3:7) complex
$(UO_2)_3(OH)_8^{2-}$	Trimer uranium (VI) hydroxide ion – (3:8) complex
$(UO_2)_3(OH)_{10}^{4-}$	Trimer uranium (VI) hydroxide ion – (3:10) complex
$(UO_2)_4(OH)_6^{2+}$	Quadrimer uranium (VI) hydroxide ion – (4:6) complex
$(UO_2)_4(OH)_7^+$	Quadrimer uranium (VI) hydroxide ion – (4:7) complex
$(UO_2)_5(OH)_8^{2+}$	Pentamer uranium (VI) hydroxide ion – (4:7) complex
UO_3	Uranium (VI) trioxide
$UO_3 \cdot 2H_2O$	Schoepite
UO_4	Uranium (VI) peroxide
WIPP	Waste Isolation Pilot Plant
XANES	X-ray Absorption Near Edge Spectroscopy
XRD	X-Ray Diffraction

Uranium (VI) Solubility in WIPP Brine

1.0 INTRODUCTION

The solubility of actinides in the VI oxidation state in Waste Isolation Pilot Plant (WIPP) brine was and continues to be considered in WIPP performance assessment (PA). Actinides that could potentially exist in the VI oxidation state are U(VI), Np(VI) and Pu(VI). Of these, only U(VI) is considered in WIPP PA because its existence cannot be completely excluded, as is the case for Np(VI) and Pu(VI), under the highly reducing conditions expected to predominate in the WIPP. Since uranium is a relatively minor contributor to overall potential release of actinides from the WIPP, a VI actinide model was never developed.

The solubility of uranium (VI) in brine systems has not been well studied and, in particular, the effect of carbonate complexation on its solubility is not well understood. For this reason, a 1 mM upper limit to its solubility is used in WIPP PA release calculations. It is in this context that the Los Alamos National Laboratory-Carlsbad Operations (LANL-CO) Actinide Chemistry and Repository Science Program (ACRSP) team performed multi-year uranium (VI) solubility experiments in simulated WIPP brine. These data, which are summarized in this report, are the first WIPP-relevant data for the solubility of U(VI) and can, in effect, be used to establish the degree of conservatism in the WIPP PA modeling assumptions.

The key objectives of this technical summary report are to provide the following:

1) An updated literature review for the solubility of uranium in the VI oxidation state under conditions that are relevant to the WIPP case.
2) A summary of the WIPP-specific data obtained by the LANL-CO/ACRSP team on the solubility of U(VI) in simulated WIPP brine. These data, more generically, apply to An(VI) solubility in the WIPP.
3) An overall assessment of the current WIPP PA assumptions in light of the literature review and our WIPP-specific results.

The WIPP is located in the Delaware Basin in southeastern New Mexico 26 miles east of Carlsbad. It is the only operating underground nuclear waste repository in the United States. It was first certified by the Environmental Protection Agency (EPA) in May 1998 as a transuranic (TRU) waste repository. The regulatory guidelines for the WIPP are given in 40CFR191/194 [DOE 1996]. Based on these regulations, the WIPP is required to undergo a re-certification process by the EPA every five years. The first Compliance Recertification Application (CRA) was submitted in 2004 by Department of Energy Carlsbad Field Office (DOE/CBFO), and was approved in April 2006. The second CRA was submitted in 2009, and approved by EPA in November 2010. The results summarized in this report will contribute to the third WIPP recertification application that will be submitted in 2014.

The WIPP-relevant solubility studies summarized in this report were performed by the LANL-CO/ACRSP team at the New Mexico State University (NMSU) Carlsbad Environmental Monitoring and Research Center (CEMRC). The overall research goals of ACRSP are 1) to establish the conservatisms of the current WIPP PA calculations of actinide solubility, 2) to help establish a more robust WIPP chemistry model, and 3) to extend past research to conditions that better simulate potential brine environments in the WIPP. This is being done by a combination of redox invariant analog studies and actinide studies in two simulated WIPP brines, GWB and ERDA-6 brine, which bracket the range of brine composition expected in the WIPP. All of the experiments are performed in compliance with the QAPD.

2.0 ROLE AND IMPORTANCE OF ACTINIDE (VI) SOLUBILITY IN CRA-2009

The role and importance of An(VI) solubility in CRA-2009 was presented in Appendix SOTERM [SOTERM 2009]. The relative importance, based on their potential to contribute to actinide release from the WIPP, of the predominant actinides and oxidation states in the WIPP is:

Importance of actinide solubility to release: Pu ≈ Am >> U > Th >> Np ≈ Cm

Importance of actinide oxidation state: An(III) > An(IV) >> An(VI) >> An(V)

In the actinide inventory for the TRU waste emplaced in the WIPP panels [Van Soest 2012], uranium is indicated to be the most prevalent actinide by mass and plutonium is the most prevalent TRU component (most of which is Pu-239). Current estimates predict that ~226 metric tons of uranium will be placed in the repository [Van Soest 2012], but this is believed to be a high estimate since uranium content in waste is often indirectly determined. From the perspective of Curie content, plutonium and americium contributions are approximately equal. Together, Pu and Am are by far the most important contributors to the potential actinide release calculations. In terms of overall actinide oxidation states, III and IV are expected to predominate in the WIPP, although it was recognized that localized oxidizing zones may exist. These transient oxidizing zones will be overwhelmed by the highly reducing environment established by the waste components (e.g., Fe from the containers) and anticipated microbiology (e.g., sulfate reduction and metal reducers).

2.1 WIPP Position on Uranium Source Term

The WIPP position on the uranium source term is addressed in the following excerpt from Appendix SOTERM [SOTERM 2009]:

SOTERM-3.3 Uranium Chemistry

*U is not a TRU component, but is, by mass, expected to be the most prevalent actinide component in the WIPP. Current estimates predict that ~647 metric tons will be placed in the repository (see Table SOTERM-7) *. By mass, greater than 99% of this U will be the ^{238}U isotope, with minor amounts of ^{233}U, ^{234}U, ^{235}U, and ^{236}U. U does not contribute significantly to the calculation of actinide release through cuttings/cavings and spallings because of its low specific activity. U release can occur through the Culebra in very small amounts because of its potentially high solubility in the VI oxidation state.*

* 647 metric tons of U estimates from [TWBIR-2004] were refined in the later PAIR-2012 document and reduced to 226 metric tons [Van Soest 2012]

> *U release, as the ^{234}U isotope, was calculated in the CRA-2004 PABC. In the WIPP PA, the oxidation state distribution assumption is that U speciates as U(IV) in 50% of the PA vectors and as U(VI) in the other 50% of the vectors. The U concentration for this oxidation state is currently set at 1 mM (U.S. Environmental Protection Agency 2005), since there is no An(VI) model in the WIPP. U(IV) solubility is calculated using the Th(IV) speciation data reported in the FMT model. For the current WIPP PA assumptions, uranium does not contribute significantly to the overall release of actinides from the WIPP.*

In summary, it is conservatively assumed in CRA-2009 Appendix SOTERM [SOTERM 2009] that uranium speciates in the IV oxidation state in 50% of the PA vectors (reduced vectors) and speciates in the VI oxidation state in the other 50% of the PA vectors (oxidized vectors). This is a conservative assumption since much lower solubility U(IV) species should be predominant under the highly reducing anoxic conditions expected in the WIPP. The solubility of U(VI) in the WIPP was conservatively set by the EPA to be 10^{-3} M to account for the lack of reliable data on the effects of carbonate complexation [EPA 2005].

2.2 CRA-2009 WIPP Position on Actinide (VI) Solubility

The actinides of interest to the WIPP that could speciate in the VI oxidation state are uranium and plutonium, and, to a much lesser extent due to inventory limitations, neptunium. Plutonium (VI) is only expected as a transient oxidation state for plutonium given the reducing conditions expected in the repository. In WIPP PA, plutonium speciates as Pu(IV) in the oxidized vectors and Pu(III) in the reduced vectors. Uranium (VI), in this context, is predicted to be the only VI actinide present in the WIPP in significant concentrations. The uranyl ion, UO_2^{2+},is the most stable of the actinyl (VI) cations [Morss 2006] towards reduction in a wide range of aqueous systems. This redox stability makes it suitable for our uranium solubility studies, although there are serious limitations in extending these results to other An(VI) actinides [SOTERM 2009]. As part of the WIPP Actinide Source Term (ASTP) program conducted in the 1990s, a range of solubilities was assigned to each probable actinide oxidation state. The goal of the ASTP was to determine the concentration of actinides present in WIPP disposal rooms that could be mobilized by contact with brine and possibly migrate from the WIPP to the accessible environment. This program featured the development of a numerical model to predict mobile actinide concentrations with order-of-magnitude accuracy. This accuracy requirement reflected the expected precision in the WIPP Performance Assessment (PA) calculations for EPA compliance [Novak 1996].

A summary of the oxidation-state specific actinide solubilities calculated for the various WIPP performance assessments is given in Table 2-1. The WIPP ASTP program, however, did not develop a model for the solubility of actinides in the VI oxidation state. Hobart and Moore estimated that the appropriate uranium (VI) concentration for Brine A and ERDA-6 brine was 1.2×10^{-5} M, based on an assessment of the limited experimental data available at the time [Hobart 1996; Brush 2003]. This value was selected because it was within the range of the available experimental values. A somewhat lower value of $8.7\text{x}10^{-6}$ M that corresponds to the solubility of schoepite ($UO_3\cdot2H_2O$) as the controlling phase [Hobart 1996] was used in the WIPP CCA , PAVT, and CRA-2004 calculations.

Table 2-1. Actinide Solubilities (M) Calculated (+III, +IV, and +V) or Estimated (+VI) for the CRA-2009 PABC, the 2004 PABC, the CRA-2004 PA, the 1997 PAVT and the CCA PA [SOTERM 2009; Brush 2009].

Actinide Oxidation State, and Brine	CRA-2009 PABC Solubilities (Hydro-magnesite, with organics, all vectors)	CRA-2004 PABC Solubilities (Hydro-magnesite, with organics, all vectors)	CRA-2004 Solubilities (Hydro-magnesite, with organics, microbial vectors)	PAVT Solubilities (Hydro-magnesite, without organics, all vectors)	CCA Solubilities (Magnesite, without organics, all vectors)
+III, Salado brine	1.66×10^{-6}	3.87×10^{-7}	3.07×10^{-7}	1.2×10^{-7}	5.82×10^{-7}
+III, Castile brine	1.51×10^{-6}	2.88×10^{-7}	1.69×10^{-7}	1.3×10^{-8}	6.52×10^{-8}
+IV, Salado brine	5.63×10^{-8}	5.64×10^{-8}	1.19×10^{-8}	1.3×10^{-8}	4.4×10^{-6}
+IV, Castile brine	6.98×10^{-8}	6.79×10^{-8}	2.47×10^{-8}	4.1×10^{-8}	6.0×10^{-9}
+V, Salado brine	3.90×10^{-7}	3.55×10^{-7}	1.02×10^{-6}	2.4×10^{-7}	2.3×10^{-6}
+V, Castile brine	8.75×10^{-7}	8.24×10^{-7}	5.08×10^{-6}	4.8×10^{-7}	2.2×10^{-6}
+VI, Salado brine	$\mathbf{1.0 \times 10^{-3}}$	$\mathbf{1.0 \times 10^{-3}}$	$\mathbf{8.7 \times 10^{-6}}$	$\mathbf{8.7 \times 10^{-6}}$	$\mathbf{8.7 \times 10^{-6}}$
+VI, Castile brine	$\mathbf{1.0 \times 10^{-3}}$	$\mathbf{1.0 \times 10^{-3}}$	$\mathbf{8.8 \times 10^{-6}}$	$\mathbf{8.8 \times 10^{-6}}$	$\mathbf{8.8 \times 10^{-6}}$

In the CRA-2004 Performance Assessment Baseline Calculation (PABC) and subsequent PA calculations a value of 10^{-3} M was used as the solubility of U(VI). This was based on recommendations by the EPA to better account for uncertainties in the effect of carbonate on the solubility of U(VI). This value of 10^{-3} M is a fixed upper-limit value that reflects the scarcity of uranium (VI) solubility data relevant to WIPP repository conditions and the lack of a thermodynamic model for An(VI) solubility.

2.3 EPA Position on Uranium (VI) Solubility

The current EPA position on uranium (VI) solubility is presented in the following excerpt from [EPA 2010, page 79-81]:

6.4.4.2 Uranium

Uranium is assumed to be present in WIPP brines as uranium (IV) in 50% of the PA realizations, and as uranium (VI) in 50% of the PA realizations (see Section 5.0). The solubility of uranium (IV) is assumed equal to the thorium (IV) solubility (Section 6.1.2). Because DOE has not developed a model for calculating the solubility of uranium (VI), a fixed bounding concentration of 10^{-3} M is assumed for PA (Section 6.3.4).

DOE (2009, Appendix SOTERM-2009) addressed the solubility and speciation of uranium (VI) (Section 3.3.1.3), and provided WIPP-specific experimental results from Lucchini et al. (2009) that have become available since the PABC04. Because this report was not provided with the CRA-2009, EPA requested a copy from DOE for review (Cotsworth 2009a, Comment 1-23-2b).This report was received from DOE (Moody 2009b), but the correct citation is Lucchini et al.(2010).

Lucchini et al. (2010) investigated the solubility of uranium (VI) solid phases in brine, using sequential addition of uranium (VI) stock solution to the brines to establish oversaturation with respect to potential uranium (VI) phases. Experiments were carried out in simulated GWB from approximately pcH 6 to 9 and in simulated ERDA-6 from approximately pcH 8 to 12. All experiments were carried out in a nitrogen atmosphere and CO_2 was excluded from the experiments. The concentrations of uranium (VI) in the carbonate-free GWB and ERDA-6 brines were approximately 10 to 100 times lower than previously reported for carbonate-free 5 M NaCl brines by Díaz Arocas and Grambow (1998). At moderately alkaline pcH values, the solubility of uranium was about one order of magnitude higher in GWB than in ERDA-6 brine (Figure 6-2 – Source: Lucchini et al. (2010), Figure 4-9).

DOE (2009, Appendix SOTERM-2009, Section SOTERM-3.3.1.3) noted the higher solubility in GWB brine compared to ERDA-6 brine, and attributed the higher solubility to complexation by higher borate and sulfate ion concentrations in GWB. In a letter sent to DOE (Cotsworth 2009a, Comment 1-23-6c), EPA observed that higher concentrations in these experiments and in neodymium solubility experiments (Section 6.4.4.5) attributable to borate complexation do not appear to be consistent with the current Dissolved Actinide Source Term conceptual model assumption that states (SC&A 2008b, Appendix A.3):

> *The important ions in WIPP brines are H^+, Na^+, K^+, Mg^{2+}, OH^-, Cl^-, CO_3^{2-}, SO_4^{2-}, and Ca^{2+}. Other ions such as PO_4^{3-}, F^-, Al^{3+}, Fe^{2+}, and Fe^{3+} may be important, but their effects are included only in a qualitative understanding of the chemical environment.*

However, borate complexation of uranium (VI), if it occurs to a significant extent, would not substantially change the current understanding of likely uranium (VI) solubility in WIPP brines because it is expected that uranyl carbonate species are likely to dominate aqueous speciation under WIPP repository conditions. DOE clarified that the potential effects of borate complexation on actinide solubilities were still under investigation, and that different solubilities predicted in GWB and ERDA-6 brine were likely caused by the many differences between the two brines and not solely by different borate concentrations (Moody 2010a). […].

Because of the probable importance of carbonate complexation on uranium (VI)

concentrations in brine under repository conditions, the experiments reported by Lucchini et al. (2010) cannot be used to revise the upper limit of 10^{-3} M established for uranium (VI) at the time of the PABC04 (Section 6.3.4). However, these experiments provide a baseline for experiments planned by DOE for uranium solids solubility in WIPP brines with carbonate.

This excerpt from the EPA documentation [EPA 2010] mostly discusses the data presented in [Lucchini 2010a], which were the only WIPP-relevant data on uranium (VI) solubility since the CCA at that time. The EPA noted that borate complexation of uranium (VI) will not significantly affect uranium (VI) solubility in WIPP brine, because of the predominance of carbonate complexation. The 1 mM solubility limit for U (VI), although it takes into account some new experimental data published in the literature since the CCA, is not based on WIPP-relevant data and conservatively overestimated the expected solubility of uranium in the WIPP.

3.0 LITERATURE BACKGROUND: SOLUBILITY OF U(VI)

The solubility and extent of aggregation in WIPP-relevant brine are key factors that define the potentially mobile concentration of actinides from an underground repository to the environment [Clark 1995, Runde 2000, Moulin 2001, Choppin 2003]. Solubility, which is the focus of this report, is governed by the oxidation state distribution and the speciation of each oxidation state.

The solubility of uranium in the VI oxidation state (U(VI)) under repository conditions is dominated by the relative contribution of hydrolysis and carbonate complexation. In the absence of carbonate, the speciation of uranium (VI) in water is dominated by hydrolysis (section 3.1). We also report on some literature experimental results that were performed to determine the solubility of uranium (VI) under conditions that approach those expected in WIPP (brine, high ionic strength, basic pC_{H^+}), in the absence of carbonate. These literature results are presented and discussed in section 3.2. Section 3.3 presents experimental work reported in the literature on the effect of carbonate on the speciation and solubility of U(VI) under salt repository conditions.

3.1 Hydrolysis of Uranium (VI)

The hydrolysis of UO_2^{2+} has been extensively studied, partially because it forms a wide variety of polynuclear hydrolytic species, resulting in a quite complex chemistry. These data were critically and extensively reviewed [Guillaumont 2003].

Hydrolysis reactions occur for the f-elements in weakly acidic to alkaline solutions in the III, IV and VI oxidation states, and often predominate over other complexation reactions in neutral and basic solutions. In particular, hydrolysis is predominant in the pH range of interest to the WIPP when other strong complexants are not present.

The hydrolysis reactions involving UO_2^{2+} can be expressed by the general reaction:

$$n\,UO_2^{2+} + q\,H_2O \Leftrightarrow \left((UO_2)_n(OH)_q\right)^{2n-q} + q\,H^+ \qquad 3\text{-}1$$

$${}^*\beta_{nq} = \left[\left((UO_2)_n(OH)_q\right)^{2n-q}\right]\left[H^+\right]^q \Big/ \left[UO_2^{2+}\right]^n \qquad 3\text{-}2$$

where $*\beta_{nq}$ increases with increasing cationic charge density. Such hydrolysis reactions can also be described as hydroxide complexation reactions:

$$n\,UO_2^{2+} + q\,OH^- \Leftrightarrow \left((UO_2)_n(OH)_q\right)^{2n-q} \qquad 3\text{-}3$$

$$\beta_{nq} = \left[\left((UO_2)_n(OH)_q\right)^{2n-q}\right] \Big/ \left[UO_2^{2+}\right]^n \left[OH^-\right]^q \qquad 3\text{-}4$$

with $K_W = [H^+][OH^-]$, this becomes

$$\beta_{nq} = {}^{*}\beta_{nq} / K_W^q \qquad 3\text{-}5$$

Palmer and Nguyen-Trung established the speciation diagram for the formation of $\left((UO_2)_n(OH)_q\right)^{2n-q}$ with $[UO_2^{2+}]_{total}$ = 4.75 × 10^{-4} M, ionic strength I = 0.1 M, T = 25 ºC (Figure 3-1) [Palmer 1995]. This diagram was obtained from fitted experimental data given in Table 3-1 by the authors.

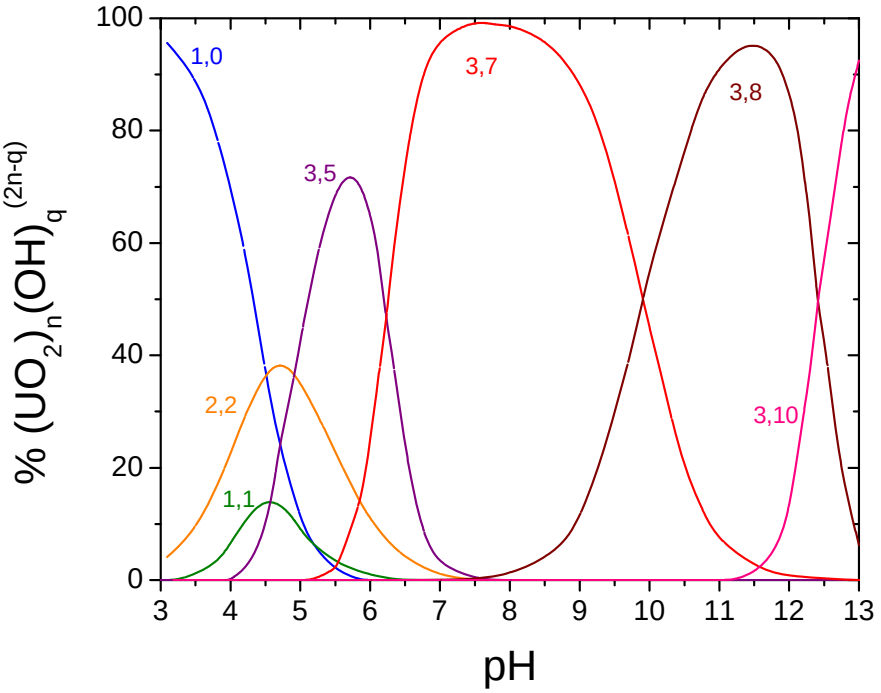

Figure 3-1. Speciation diagram for the formation of $\left((UO_2)_n(OH)_q\right)^{2n-q}$ with $[UO_2^{2+}]_{total}$ = 4.75 × 10^{-4} M, ionic strength I = 0.1 M, T = 25 ºC. The number pairs shown on the graph refer to n and q. (Based on data in Palmer 1995)

Table 3-1. Hydrolysis constants at Ionic Strength (I) = 0 and 25ºC for the formation of $((UO_2)_n(OH)_q)^{2n-q}$ species .

n,q	log $*\beta^o_{nq}$ [Palmer 1995]	log $*\beta^o_{nq}$ [Guillaumont 2003]
1,1	-5.42 ± 0.04[a]	-5.25 ± 0.24
2,2	-5.51 ± 0.04	-5.62 ± 0.04
3,5	-15.33 ± 0.12	-15.55 ± 0.12
3,7	-27.77 ± 0.09	-32.2 ± 0.8
3,8	-37.65 ± 0.14	---
3,10	-62.4 ± 0.3	---

[a] For I = 0.10 M (KNO_3).

In very dilute solutions where $[UO_2^{2+}] \leq 10^{-6}$ M, the hydrolysis of UO_2^{2+} first forms mononuclear $UO_2(OH)_q^{2-q}$ species, but above this concentration, UO_2^{2+} exists mainly as polynuclear species [Morss 2006]. At pH values between 5 and 6.5, the 3:5 complex $(UO_2)_3(OH)_5^+$ is prominent. Between pH = 6.5 and 9.5, the uranyl cation is almost exclusively in the form of the 3:7 complex $(UO_2)_3(OH)_7^-$. At $9.5 \leq pH \leq 12.5$, the uranyl cation is present in carbonate-free solution as the 3:8 complex $(UO_2)_3(OH)_8^{2-}$. The uranyl complex $(UO_2)_3(OH)_{10}^{4-}$ is expected at $pH \geq 12.5$.

Other hydrolytic uranyl species were reported to exist [Morss 2006]. In chloride solutions, $(UO_2)_3(OH)_4^{2+}$ is also formed. In concentrated solutions at low pH, $(UO_2)_2OH^{3+}$ may be present. Other complexes which have been proposed to form are $(UO_2)_3(OH)_7^-$, $(UO_2)_3(OH)_{10}^{4-}$, $(UO_2)_4(OH)_6^{2+}$, $(UO_2)_4(OH)_7^+$ and $(UO_2)_5(OH)_8^{2+}$. The existence of the dimer $(UO_2)_2(OH)_2^{2+}$ has been confirmed by direct determination of the species present in hydrolyzed uranyl (VI) chloride solutions [Åberg 1970]. However, for the expected WIPP conditions, and in the absence of major complexants (such as carbonate), the speciation of the uranyl cation should be a mixture of the 3:7 and 3:8 hydrolytic complexes.

3.2 Solubility of Uranium (VI) in Carbonate-free Brine

In this section, we present and discuss the uranium literature data in brine systems that were obtained in reported carbonate-free media. Overall, there are few/no uranium (VI) solubility data that are directly relevant to WIPP-specific conditions: i.e., magnesium-sodium-chloride brines, high ionic strength (I > 5 M), and moderately alkaline pH. The available results in the more generic brine systems are summarized in Table 3-2 and plotted in Figure 3-2.

Yamazaki *et al.* conducted U(VI) solubility experiments from both oversaturation and undersaturation in a synthetic brine at pC_{H+} values ranging from 6.4 to 12.4 [Yamazaki 1992]. The composition of this synthetic brine was close to the composition of the WIPP GWB brine, but with higher concentrations of NaCl, NaBr, KCl and $MgCl_2$ and an ionic strength ~6 M. This synthetic brine initially contained 0.11 mM of bicarbonate (HCO_3^-), but the solution treatment (continuous nitrogen gas flow above the solution) likely removed some of the carbonate from solution before the later uranium additions, and probably prevented any CO_2 uptake during the experiment. The results obtained at the pC_{H+} closest to WIPP repository conditions with no further carbonate additions are listed in Table 3-2 and plotted in Figure 3-2.

Table 3-2. Experimental uranium (VI) solubility data in carbonate-free high ionic strength media.

U (VI) concentration (M)	pC_{H+}	Solution	Time (days)	Solid	Reference
$(2.8\pm1.8)\times10^{-5}$	8.9	5 M NaCl	≈ 50	$Na_{0.68}UO_{3.34}\cdot(2.15\pm0.10)\ H_2O$	[Diaz-Arocas 1998]
$(8.2\pm4.6)\times10^{-5}$	7.6	5 M NaCl	≈ 110	$Na_{0.45}UO_{3.23}\cdot(4.5\pm0.1)\ H_2O$	[Diaz-Arocas 1998]
$(4.2\pm1.9)\times10^{-4}$	7.1	5 M NaCl	≈ 170	$Na_{0.29}UO_{3.15}\cdot(2.9\pm0.2)\ H_2O$	[Diaz-Arocas 1998]
$(2.8\pm0.9)\times10^{-3}$	6.5	5 M NaCl	≈ 170	$Na_{0.14}UO_{3.07}\cdot(2.5\pm0.1)\ H_2O$	[Diaz-Arocas 1998]
2.8×10^{-6}	~10.8	WIPP brine	Not specified	$UO_2(OH)_2$	[Palmer 1996]
$(1.82\pm0.01)\times10^{-3}$	8.4	Brine (air atmosphere) ~6 M	100	α-schoepite (oversaturation)	[Yamazaki 1992]
$(1.81\pm0.01)\times10^{-3}$	8.4	Brine (air atmosphere) ~6 M	100	α-schoepite (oversaturation)	[Yamazaki 1992]
$(1.40\pm0.05)\times10^{-3}$	8.4	Brine (air atmosphere) ~6 M	244	α-schoepite (undersaturation)	[Yamazaki 1992]
$(1.80\pm0.05)\times10^{-3}$	8.4	Brine (air atmosphere) ~6 M	244	α-schoepite (undersaturation)	[Yamazaki 1992]
$(3.8\pm0.4)\times10^{-7}$	10.4	Brine ~6 M (initial 0.11mM HCO_3^-)	150	$Mg(OH)_2$ and $K_2U_2O_7$ (oversaturation)	[Yamazaki 1992]
$(3.1\pm0.3)\times10^{-7}$	10.4	Brine ~6 M (initial 0.11mM HCO_3^-)	150	$Mg(OH)_2$ and $K_2U_2O_7$ (oversaturation)	[Yamazaki 1992]

Uranium (VI) concentrations of approximately 10^{-7} M were observed at pC_{H+} = 10.4 and 12.4 when nitrogen gas was continuously passing over the solutions to minimize CO_2 uptake. Despite extensive precipitation of brucite $Mg(OH)_2$ at these high pC_{H+} values, the solubility-controlling phase at $pC_{H+} \geq 9.3$ was found to be potassium diuranate $K_2U_2O_7$.

At pH = 9.8 in brine in the absence of carbonate (estimated pC_{H+} ~10.8), Palmer observed a U(VI) solubility of 2.8×10^{-6} M in equilibrium with a phase that appeared to be $UO_2(OH)_2$ (s) [Palmer 1996]. These results were privately communicated by Palmer, and reported by Hobart [1996], but never published. For this reason they are not considered further in this report.

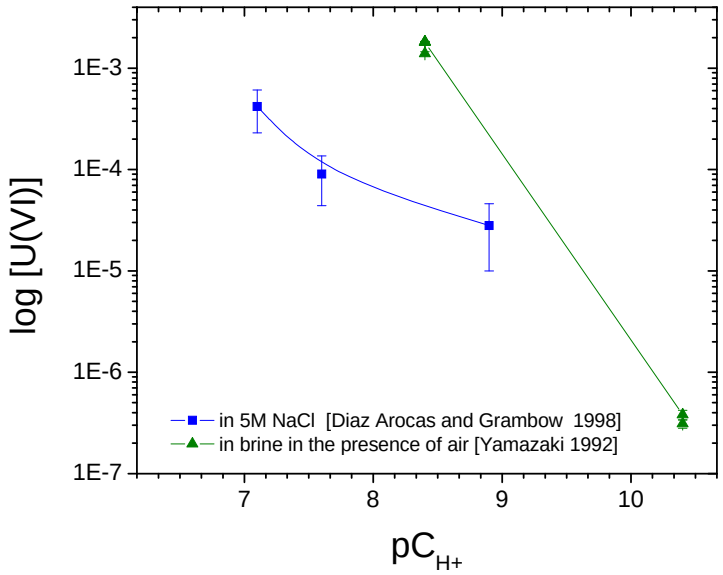

Figure 3-2. Uranium (VI) solubility data obtained in carbonate-free (otherwise mentioned) high ionic strength media at $pC_{H+} > 7$. The full square symbols and corresponding trend line represent data obtained by Diaz Arocas and Grambow in 5 M NaCl under an argon atmosphere [Diaz Arocas 1998]. The full triangle symbols and corresponding trend line represent data obtained by Yamazaki *et al.* in brine (I~6 M) with an air atmosphere [Yamazaki 1992].

Diaz-Arocas and Grambow investigated uranium (VI) solubility in NaCl solutions up to 5 M at 25 °C and different basic pH values, under an argon atmosphere using an oversaturation approach [Diaz-Arocas 1998]. Their uranium concentration equilibria in 5 M NaCl are presented in Table 3-2. It should be noted that the published values were converted from molality values to molarity using a density value of 5 M NaCl equal to 1185 g/L. Poorly-crystalline sodium-uranates, identified by XRD, were reported as the solubility-controlling phases with a solubility of about 3×10^{-5} M at pC_{H+} = 8.9 in 5 M sodium chloride in the absence of carbonate.

The uranium solubility reported by Diaz-Arocas and Grambow was about two orders of magnitude lower than the data obtained by Yamazaki at a comparable pC_{H+} value (~8.4).

It is difficult to provide an explanation for this difference since there were a number of differences between these two sets of experiments. The Yamazaki experiments may have had some residual carbonate in their system and were done in the presence of oxygen. In the Yamazaki oversaturation experiments at pC_{H+} = 8.4 and an air atmosphere, a poorly crystalline solid phase, identified as α-schoepite $UO_3 \cdot 2H_2O$, was identified as the uranium solubility controlling phase [Yamazaki 1992]. He also found that the equilibration time was much longer at pC_{H+} = 10.4 than at lower pC_{H+}, which likely reflected the much slower uranium phase transformation that may have occurred in his experimental approach.

3.3 Solubility of Uranium (VI) in Brine in the Presence of Carbonate

In contrast to the carbonate-free case, there are several WIPP-relevant studies reported in the literature that were performed in the presence of carbonate [Kramer-Schnabel 1992, Reed 1997, Lin 1998, Yamamura 1998, Fanghanel 2002]. The role of carbonate (CO_3^{2-}) in the uranium (VI) solubility is indeed important [Clark 1995, Guillaumont 2003]. Carbonate complexes of uranium are of interest not only in nuclear waste repository chemistry, but also in industry because of extensive applications, primarily in recovery from ores and nuclear fuel reprocessing. The alkaline leaching process for the recovery of uranium is very selective and utilizes the high stability of the soluble 1:3 complex, $UO_2(CO_3)_3^{4-}$, as a means of selectively separating uranium from ore. Recovery of the uranium from the leach liquor is achieved either by addition of hydroxide to precipitate $Na_2U_2O_7$, or by acidification to liberate carbon dioxide [Clark 1995].

In the absence of other complexing ligands, carbonate complexation will dominate the speciation of the uranyl ion under near-neutral pH conditions as long as there is ample carbonate-bicarbonate available [Clark 1995]. Complexation constants for binary U(VI) carbonate complexes at I = 0 M and 25ºC are listed in Table 3-3 [Guillaumont 2003]. Three monomeric complexes, $UO_2(CO_3)$, $UO_2(CO_3)_2^{2-}$, and $UO_2(CO_3)_3^{4-}$ are predicted to be present. There is also evidence from redox, solubility, and spectroscopy data supporting the existence of polynuclear species of formulas $(UO_2)_3(CO_3)_6^{6-}$, $(UO_2)_2(CO_3)(OH)_3^{-}$, and $(UO_2)_{11}(CO_3)_6(OH)_{12}^{2-}$, which can form only under conditions of high metal ion concentration or high ionic strength [Clark 1995]. At uranyl concentrations above 10^{-3} M, the trimeric cluster $(UO_2)_3(CO_3)_6^{6-}$ is present in significant concentrations. When the uranyl ion concentration exceeds the carbonate concentration, hydrolysis competes with carbonate complexation and plays an increasingly important role [Clark 1995].

The major uranyl carbonato complex in solution at low ionic strength and high carbonate concentration is $UO_2(CO_3)_3^{4-}$ [Kramer-Schnabel 1992, Peper 2004]. However, at I = 0.5 M and I = 3 M, the polynuclear species $(UO_2)_3(CO_3)_6^{6-}$ becomes an important competitor of $UO_2(CO_3)_3^{4-}$. Grenthe *et al.* indicated that the formation of $(UO_2)_3(CO_3)_6^{6-}$ is favored at high ionic strengths due to possible stabilization of the complex by ions of the background electrolyte [Grenthe 1984]. The experimental curve of the solubility of UO_2CO_3 obtained by Kramer-Schnabel *et al.* is displayed in Figure 3-3, together with two curves obtained at higher ionic strengths by Grenthe *et al.* [Grenthe 1984]. The experimental points from Kramer-Schnabel *et al.* were obtained in the region $3 < pH < 6$ and $-11 < \log[CO_3^{2-}] < -6$ where UO_2CO_3 is the solid phase. These experimental data were fit using the stability constants of the following three carbonate complexes: UO_2CO_3, $UO_2(CO_3)_2^{2-}$ and

$UO_2(CO_3)_3^{4-}$. Including additional uranyl-carbonate complexes did not improve the fit obtained. An important observation from Figure 3-3 is that uranium concentration in solution exhibited an increasingly complex dependency on ionic strength with increasing carbonate concentrations.

Table 3-3. Complexation constants for binary U(VI) carbonate complexes at I = 0 M and 25°C [Guillaumont 2003].

Reaction and Solubility product for UO_2CO_3(cr)	
$UO_2CO_3(cr) \rightleftharpoons UO_2^{2+} + CO_3^{2-}$	Log $K^0_{SP(cr)}$=-14.76 ± 0.02
Reactions and Formation constants β^0_{nq} for $(UO_2)_n(CO_3)_q^{2n-2q}$	
$UO_2^{2+} + CO_3^{2-} \rightleftharpoons UO_2CO_3(aq)$	Log β^0_{11}=9.94 ± 0.03
$UO_2^{2+} + 2\ CO_3^{2-} \rightleftharpoons UO_2(CO_3)_2^{2-}$	Log β^0_{12}=16.61 ± 0.09
$UO_2^{2+} + 3\ CO_3^{2-} \rightleftharpoons UO_2(CO_3)_3^{4-}$	Log β^0_{13}=21.84 ± 0.04
$3\ UO_2^{2+} + 6\ CO_3^{2-} \rightleftharpoons (UO_2)_3(CO_3)_6^{6-}$	Log β^0_{36}=54.0 ± 1.0

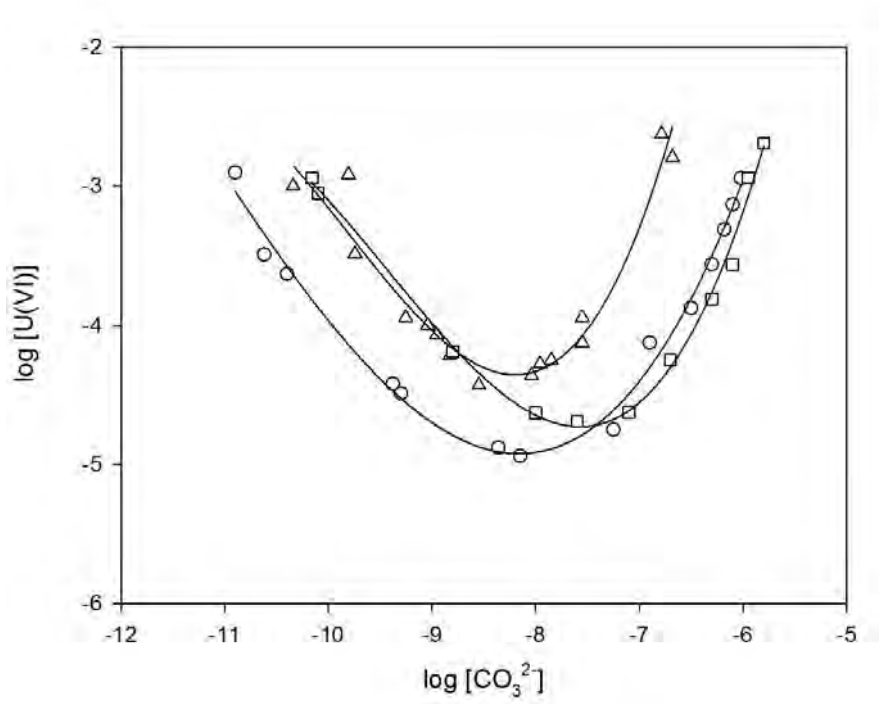

Figure 3-3. Experimental (symbols) and theoretical (lines) solubility curves of UO_2CO_3 at 25ºC and I = 0.1M (triangles, [Kramer-Schnabel 1992]), I = 0.5 M (squares, [Grenthe 1984]) and I = 3 M (circles, [Grenthe 1984]).

At high pH, Yamamura *et al.* demonstrated that hydrolysis overwhelms the carbonate complexation when carbonate source is limited [Yamamura 1998]. The solubility of U(VI)

was measured in highly basic solutions ($11 \leq$ pH ≤ 14) at different ionic strengths (0.5 – 2 M) over a wide range of carbonate concentrations (10^{-3} – 0.5 M) using both oversaturation and undersaturation approaches. In the oversaturation experiments, the solubility of U(VI) decreased with increasing equilibration time from 1 week to 1 year, suggesting an increase in the crystallinity of the solid phase with aging. The solid phase was identified as $Na_2U_2O_7.xH_2O$ by X-ray diffraction. The undersaturation experiments, which were conducted for one month with the solid phase, indicated a rapid equilibrium. These data were well interpreted by considering the formation of $UO_2(OH)_3^-$, $UO_2(OH)_4^{2-}$ and $UO_2(CO_3)_3^{4-}$ [Yamamura 1998].

The influence of carbonate on U(VI) solubility in highly saline solution was investigated by Yamazaki *et al.* [1992], Lin *et al.* [1998] and Reed *et al.* [1997].

A few U(VI) solubility experiments performed by Yamazaki *et al.* were conducted in a synthetic brine and an air atmosphere [Yamazaki 1992]. This implies that some carbonate was present in solution, as a result of the equilibrium with carbon dioxide from the ambient atmosphere. The results obtained at $pC_{H+} = 8.4$ using both oversaturation and undersaturation approaches are listed in Table 3-2 and plotted in Figure 3-2. A good agreement was found between uranium (VI) solubility in the oversaturation and undersaturation experiments that were carried out in an air atmosphere. At this pC_{H+} value, millimole concentrations of uranium were measured in solution. Solids obtained at $pC_{H+} = 8.4$ were identified as poorly crystalline schoepite ($UO_3 \cdot xH_2O$) by X-Ray Diffraction (XRD). Yamazaki carried out some calculations to model the competition between calcium and magnesium for carbonate complexation in order to interpret his experimental solubility data. He concluded that the uranium solubility decrease above $pC_{H+} = 8.4$ was related to a shift from the triscarbonato uranyl complex $UO_2(CO_3)_3^{4-}$ to the uranyl hydroxide complexes $UO_2(OH)_n^{2-n}$, as precipitation of calcium carbonate ($CaCO_3$) occurred, and to the conversion of schoepite to potassium diuranate.

Lin *et al.* [1998] evaluated uranium (VI) solubilities in up to 5 M NaCl, and over a range of carbonate concentrations. At carbonate ion concentrations greater than 10^{-7} M, $UO_2(CO_3)_3^{4-}$ was the dominant U(VI) complex in solution. At higher carbon dioxide partial pressures, the solubility-controlling solid phase was found to be UO_2CO_3(s), whereas at lower partial pressures, sodium uranate was identified as the solid phase in NaCl-saturated solutions. The reported solubility of UO_2CO_3(s) at a carbonate ion concentration of 10^{-5} M was approximately 5×10^{-3} M [EPA 2010]. However, in this study, the pH of the solution was not reported.

The only U(VI) solubility values available in the literature that were obtained in the presence of carbonate and that are relevant to the WIPP were featured in the fiscal year 1997 year-end report by Reed *et al.* titled, "Actinide Stability/Solubility in Simulated WIPP Brines." [Reed 1997]. The experiments were carried out in ERDA-6 brine at pH 8 (pC_{H+} ~9) and 10 (pC_{H+} ~11), and in G-Seep brine at pH 5 (pC_{H+} ~6.2) and 7 (pC_{H+} ~8.2). U(VI), Np(VI), and Pu(VI) were added to the brine samples. Carbonate (10^{-4} M) was also added to some of the samples. The experiments were conducted under a hydrogen atmosphere at 25 ± 5 °C. Concentrations and oxidation states of the actinides were monitored over time. The U(VI) concentration was stable at approximately 1×10^{-4} M when measured as a function of time in ERDA-6 brine at pH 10 (pC_{H+} ~11) in the presence of CO_3^{2-} [Reed 1997].

4.0 WIPP-RELEVANT EXPERIMENTAL RESULTS: SOLUBILITY OF UO_2^{2+} IN SIMULATED WIPP BRINE

The LANL-CO/ACRSP team performed experiments to determine the solubility of uranium (VI) in simulated WIPP brines. The data obtained from these experiments are summarized in this section. These data are the first of their kind to be generated under an approved WIPP Quality Assurance Program for the solubility of uranium (VI) in simulated WIPP brine under repository conditions.

4.1 Experimental Goals and Test Matrices

The most important goals of the solubility studies were:

- Establish the effective long-term solubility of U(VI) in brine under experimental conditions that simulate the expected environment in the WIPP.
- Strengthen the current WIPP position on An (VI) solubility under WIPP-relevant conditions.
- Evaluate the importance and relative contribution of hydrolysis and carbonate complexation to the solubility of uranium (VI) over a broad range of pC_{H+}.

The experiments described herein were performed under the Test Plan entitled "Solubility/Stability of Uranium (VI) in WIPP Brines", designated LCO-ACP-02. This Test Plan consisted of the following three tasks:

Task 1: Solubility of U(VI) in WIPP brine
Task 2: Redox stability of U(VI) in WIPP brine
Task 3: Effect of radiolytic products on uranium speciation

The solubility experiments discussed herein pertain to experiments identified in Task 1. Results from Task 2 and Task 3 are not discussed in this report.

All of the experiments described herein were performed under anoxic conditions in a nitrogen controlled atmosphere. The glovebox atmosphere was free of oxygen and carbon dioxide. Carbonate is known to have a significant impact on U(VI) solubility in the environment, whereas oxygen should not impact the aqueous speciation of U(VI), although there is a possibility that the presence of oxygen may affect solid phase formation.

In sections 4.1.1 to 4.1.3, the experimental goals and experimental matrices associated with the three key subtasks in Task 1 are presented.

4.1.1 Subtask 1: U(VI) solubility in an anoxic atmosphere

In Subtask 1, the solubility of U(VI) was investigated in carbonate-free simulated WIPP brines GWB and ERDA-6, as a function of pC_{H+}, under an anoxic atmosphere, and from over-saturation. The goal of these experiments was to evaluate the effect of hydrolysis on uranium solubility. These results defined a "baseline" carbonate-free uranium solubility that was used to evaluate the effect of carbonate on uranium (VI) solubility in subsequent studies.

Table 4-1 shows the experimental matrix for Subtask 1.

Table 4-1. Experimental matrix for carbonate-free uranium (VI) solubility studies in anoxic atmosphere using the over-saturation approach (Subtask 1).

	Brine and experimental conditions	
pC_{H+}	GWB anoxic	ERDA-6 anoxic
~6.0	TI-GW-6.x	
~7.0	TI-GW-7.x	
~8.0	TI-GW-8.x	TI-ER-8.x
~9.0	TI-GW-9.x	TI-ER-9.x
~10.0		TI-ER-10.x
~11.0		TI-ER-11.x
~12.0		TI-ER-12.x

Where x is either 0 or 1. It is the numbering of replicate experiments.

The initial results for Subtask 1 were previously presented and discussed in the LCO-ACP-10 report [Lucchini 2010a] entitled: "Actinide (VI) Solubility in Carbonate-free WIPP Brine: Data Summary and Recommendations", and in peer-reviewed publications [Lucchini 2007, 2010b, 2013]. They are reproduced herein (section 4.3.1).

4.1.2 Subtask 3: Carbonate effects study on U(VI) solubility

The effect of carbonate on U(VI) solubility was investigated in Subtask 3. Experiments were performed from over-saturation in simulated WIPP brines GWB and ERDA-6 under an anoxic atmosphere. The brines were prepared to contain defined amounts of carbonate at the start of the experiments, at different pC_{H+} values. The goal of these

experiments was to evaluate the effect of carbonate on uranium (VI) solubility as a function of pC_{H+}.

Table 4-2 shows the experimental matrix for Subtask 3. The experimental matrix takes into consideration the chemical stability of the brines as a function of pC_{H+} (see section 4.2.2).

Table 4-2. Experimental matrix to evaluate the effect of carbonate on uranium (VI) solubility (Subtask 3).

pC_{H+}	GWB Carbonate concentration (M)			ERDA-6 Carbonate concentration (M)		
	Zero	~10^{-4}	~10^{-3}	Zero	~10^{-4}	~10^{-3}
~7.5	T3-GW-CO-7.x	T3-GW-C4-7.x	T3-GW-C3-7.x			
~9.0	T3-GW-CO-9.x	T3-GW-C4-9.x	T3-GW-C3-9.x	T3-ER-CO-9.x	T3-ER-C4-9.x	T3-ER-C3-9.x
~12.0				T3-ER-CO-12.x	T3-ER-C4-12.x	T3-ER-C3-12.x

Where x is either 0 or 1. It is the numbering of replicate experiments.

4.1.3 Subtask 8: U(VI) solubility in brine from under-saturation

Solubility data are strengthened when the two experimental approaches, over-saturation and under-saturation, give similar results. Experiments in Subtask 1 were performed using the over-saturation approach. Complimentary experiments were performed in Subtask 8 in carbonate-free simplified WIPP brine, as a function of pC_{H+}, under an anoxic atmosphere, but using the under-saturation approach. Four different uranium solid phases were used: uranium peroxide, uranium trioxide, uranium hydroxide, and precipitates recovered from the over-saturation experiments.

The goal of the experiments planned in Subtask 8 was (1) to confirm the data obtained in Subtask 1 on the uranium (VI) solubility in carbonate-free brines at different pC_{H+} values, and (2) to investigate the solubility of various uranium solid phases under those experimental conditions.

Table 4-3 shows the experimental matrix for Subtask 8.

Table 4-3. Experimental matrix for uranium (VI) solubility studies in an anoxic atmosphere using the under-saturation approach (Subtask 8).

pC_{H+}	GWB brine			
	Uranium peroxide	Uranium trioxide	Uranium hydroxide	Experimental uranium precipitate
~6	T8-GWP-6.x	T8-GWT-6.x	T8-GWH-6.x	T8-GWE-6.x
~7	T8-GWP-7.x	T8-GWT-7.x	T8-GWH-7.x	T8-GWE-7.x
~8	T8-GWP-8.x	T8-GWT-8.x	T8-GWH-8.x	T8-GWE-8.x
~9	T8-GWP-9.x	T8-GWT-9.x	T8-GWH-9.x	T8-GWE-9.x
pC_{H+}	ERDA-6 brine			
	Uranium peroxide	Uranium trioxide	Uranium hydroxide	Experimental uranium precipitate
~7	T8-ERP-7.x	T8-ERT-7.x	T8-ERH-7.x	T8-ERE-7.x
~8	T8-ERP-8.x	T8-ERT-8.x	T8-ERH-8.x	T8-ERE-8.x
~10	T8-ERP-10.x	T8-ERT-10.x	T8-ERH-10.x	T8-ERE-10.x
~11	T8-ERP-11.x	T8-ERT-11.x	T8-ERH-11.x	T8-ERE-11.x
~12	T8-ERP-12.x	T8-ERT-12.x	T8-ERH-12.x	T8-ERE-12.x

Where x is either 0 or 1. It is the numbering of replicate experiments.

4.2 Experimental Approach, Limitations, Considerations, and Error Analysis

The experimental approach used in these U(VI) solubility studies is described in section 4.2.1. The limitations and constraints on the experiments performed and the overall experimental error are discussed in sections 4.2.2 and 4.2.3, respectively.

4.2.1 Experimental Approach

In Subtasks 1and 3, the general experimental approach was to investigate uranium (VI) solubility from over-saturation, as described by Nitsche [1992]. This consisted of

sequentially adding dissolved uranium until precipitation was observed. Subsequently, the uranium concentration was monitored over time until a steady-state concentration was achieved.

In Subtask 8, the general experimental approach was to investigate uranium (VI) solubility from under-saturation. This consisted of adding a pre-determined amount of uranium solid phase, until a steady-state concentration of uranium in solution was observed.

The general initial conditions of the study were:

- WIPP simulated brines
- pC_{H+} between 6 and 12
- Absence or presence of a defined amount of carbonate in the brine
- Anoxic and carbonate-free atmosphere in a nitrogen glovebox
- Temperature of 25 ± 4 ^{o}C

The overall experimental protocol used in the U(VI) solubility experiments was the following:

1) Two WIPP simulated brines (GWB and ERDA-6) were prepared according to procedure ACP-EXP-001: “Brine Preparation”. These were prepared at a 95% strength to minimize salt precipitation during the solubility experiments, at least before the pH adjustment.
2) The pC_{H+} of the brine was varied as an experimental parameter. Brine pC_{H+} was determined according to procedure ACP-EXP-010: “Determination of Hydrogen Ion Concentration in Brines”.
3) In Subtask 3, the addition of carbonate in the matrix solutions was performed using an appropriate volume of carbonate-spiked brine.
4) Concerning the over-saturation experiments, the uranyl stock solution was prepared with high oxidation-state purity in aqueous solution at pH ~ 3. For the under-saturation experiments, the uranium solid phases used in the experiments were also prepared in the laboratory using a similar high oxidation-state purity uranyl stock solution.
5) All controlled-atmosphere experiments were performed in a nitrogen glove box to eliminate any possible carbon dioxide uptake in the system and simulate the expected anoxic conditions in the WIPP. The gas phase environment (nitrogen) was monitored throughout the experiment by an oxygen analyzer (detection limit: 0.1 ppm O_2) that would detect air intrusion in the glovebox. Therefore, the CO_2 content of the nitrogen glove box was expected to be negligible (<0.2 ppb CO_2).
6) Throughout the solubility experiments, aliquots were taken, centrifugated, and filtered through Microcon® Millipore centrifugal filters with a nominal molecular weight limit of 30,000 Daltons (~10 nm pore size). Filtrates were analyzed for uranium content by Inductively Coupled Plasma-Mass Spectrometry (ICP-MS).

7) Concerning the over-saturation experiments, the subsequent additions of uranyl eventually led to its precipitation as a solid. The characterization of these uranium solid phases is a difficult task due to the low amount of solid formed and the multiphase, and usually amorphous, nature of the precipitates given the complexity of the simulated brines.

A more detailed description of some key aspects of the experimental approach is provided in the following sections.

Simulated brines used and their preparation

Two simulated WIPP brines were used in our studies. Generic Weep Brine (GWB) is a high magnesium brine that simulates the weep brine observed in the WIPP and is considered the most relevant to repository interactions due to the MgO content. Energy Research and Development Administration Well 6 brine (ERDA-6) is a low magnesium brine that simulates brine from the Castile Formation underlying the WIPP. The nominal compositions of these two simulated WIPP brines were established by Brush [1990]. We prepared and used these two brines at 95% of their initial formulation to minimize salting and to simplify the sampling process. The composition and the density of the simulated brines are given in Table 4-4.

All chemicals in these experiments were reagent-grade certified ACS (> 99% purity), and had been purchased from Fisher, with the exception of sodium tetraborate $Na_2B_4O_7$, which was obtained from Acros Organics. They were used without further purification. Appropriate amounts of salts were dissolved in high purity (HP) 18 MΩ·cm water to prepare GWB brine and ERDA-6 brine.

Table 4-4. Composition and density of GWB and ERDA-6 simulated WIPP brines (95% initial formulation).

Component	**GWB brine** [M]	**ERDA-6 brine** [M]
Na^+	3.310	4.620
Mg^{2+}	0.953	0.018
K^+	0.438	0.092
Ca^{2+}	0.013	0.011
Li^+	0.004	--
Br^-	0.025	0.010
$B_4O_7^{2-}$	0.037	0.015
Cl^-	5.250	4.410
SO_4^{2-}	0.167	0.159
Density (g/mL)	1.216	1.183
Ionic strength (M)	6.839	4.965

Carbonate-free simulated WIPP brines

Significant care was taken to establish carbonate-free conditions. Polypropylene bottles were placed in an anoxic carbon dioxide-free glovebox for two weeks to remove residual carbon dioxide (CO_2). The removal of carbonate from the brines was a two-step process. The first step consisted of acidification of the brines to $pC_{H+} \sim 3$, which converted carbonate into carbonic acid, in equilibrium with small amount of bicarbonate, then into dissolved carbon dioxide gas. The second step was to place the solutions in a vacuum chamber where they underwent for a slow pump-down process to smoothly remove all dissolved gas from the brines. The vacuum chamber was placed in a low flow-through high-purity nitrogen glove box to maintain low levels of carbon dioxide. The oxygen level in this nitrogen glove box was continuously monitored, and was always less than 10 ppm O_2, so less than 0.02 ppm of CO_2 could be present.

After more than 10 days of degassing in the vacuum chamber, the solutions were transferred to our MBraun® nitrogen glove box with an anoxic carbon dioxide-free atmosphere (high purity nitrogen). The glove box was controlled by a recirculating closed-loop oxygen purification system to ensure an anoxic, carbon dioxide-free high purity nitrogen atmosphere for the duration of the solubility experiments. The bottles were kept sealed and only opened briefly to take samples in the glovebox.

Hydrogen ion concentration and pC_{H+}

In our high ionic-strength brines (I > 5 M), the measurement of the hydrogen ion concentration is problematic due to activity coefficient effects and high sodium content. This is somewhat circumvented by using a Gran titration approach, as suggested by Rai [Rai 1995], which leads to the following relationship:

$$pC_{H+} = pH_{obs} + K \qquad 4\text{-}1$$

Here, pC_{H+} is the negative logarithm of the hydrogen concentration in molarity (mol/L or M) units, pH_{obs} is the measured/ observed pH, and K is an experimentally determined pH correction factor constant. The values of K were linearly proportional to the solution ionic strength (Figure 4-1). The values of K for the two WIPP brines used in the present work were (1.23 ± 0.01) for GWB brine and (0.94 ± 0.02) for ERDA-6, respectively [Borkowski 2009]. The pH correction values (K) for diluted brines used in the different subtasks were determined by interpolation of the linear fitting curve on Figure 4-1 and are reported in Table 4-5.

The pH of each brine solution was measured in the nitrogen glovebox with a sealed Orion-Ross combination glass electrode calibrated against NIST-certified pH buffers. Adjustments of pH to obtain the desired pC_{H+} were made with ACS certified hydrochloric acid and/or low carbonate sodium hydroxide (50 weight %) to minimize the re-introduction of carbonate. The uncertainty in the pH measurements was ± 0.1 pH unit. 50 mL-duplicates were prepared for each pC_{H+}-adjusted brine.

From this point, all brine solutions were kept in polypropylene bottles and tightly capped throughout the experiment except during sampling.

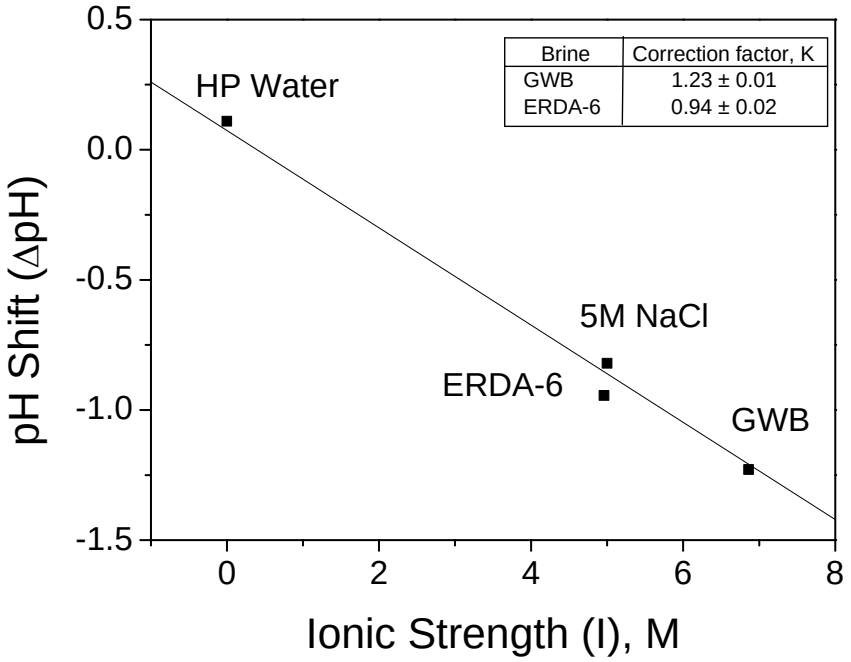

Figure 4-1. Correlation between the pH shift (ΔpH) and the ionic strength (I) of the two simulated WIPP brines, GWB and ERDA-6, 5 M NaCl brine, and high purity (HP) water. The opposite slope value of ΔpH corresponds to the correction factor K. Based on this graph, the correction factors for WIPP brines, GWB and ERDA-6, are given in the table insert [Borkowski 2009].

Table 4-5. Correction factor K as a function of ionic strength I (M).

Ionic strength (I), M	K
6.84 (GWB)	1.23
5 (5M NaCl)	0.88
4.97 (ERDA-6)	0.94
3.4	0.56
3	0.48
1	0.09
0.1	-0.08

Addition of carbonate (Subtask 3 only)

The addition of carbonate to the GWB or ERDA-6 brine in Subtask 3 was performed using a spike volume of a concentrated carbonate solution. This intermediate carbonate solution was prepared by dissolving a known amount of sodium carbonate (Na_2CO_3 - Fisher) in a determined volume of brine. An appropriate volume of the intermediate carbonate solution was then added to the GWB or ERDA-6 brine in Subtask 3 to achieve the desired carbonate concentration in solution (see experimental matrix – Table 4-2). In this way, the addition of carbonate in the Subtask 3 solutions was about 1% in volume, and dilution effects were negligible.

Uranyl solution

Our source of uranyl ion in this experiment was a uranium chloride stock solution (~ 0.15 M) that was prepared with high oxidation-state purity. Depleted uranium (VI) nitrate hexahydrate, $UO_2(NO_3)_2 \cdot 6H_2O$, was converted to a nitrate-free hydrochloric acid solution by the following consecutive steps:

- dissolution of the uranyl nitrate salt in 1 M hydrochloric acid and taking to dryness three times,
- precipitation of a uranyl hydroxide with sodium hydroxide,
- washing of the precipitate with hydroxide base to remove the residual nitrate impurities,
- and finally re-dissolution of the precipitate in 1 M hydrochloric acid.

Prepared this way, the uranium stock solution (~ 0.15 M) had an oxidation-state purity of ~100% for UO_2^{2+} (Figure 4-2). Appropriate amounts of this U(VI) stock solution were volumetrically pipetted into an aliquot of each brine at a pH of ~ 3-4 and checked for precipitation. This step led to properly diluted carbonate-free solutions to use as uranyl spikes in the pC_{H+}-adjusted brines.

The uranyl stock solution was stored in a polypropylene bottle, tightly capped, in room atmosphere. No uptake of carbon dioxide over time in the uranyl stock solution was expected, considering the acidity of the solution.

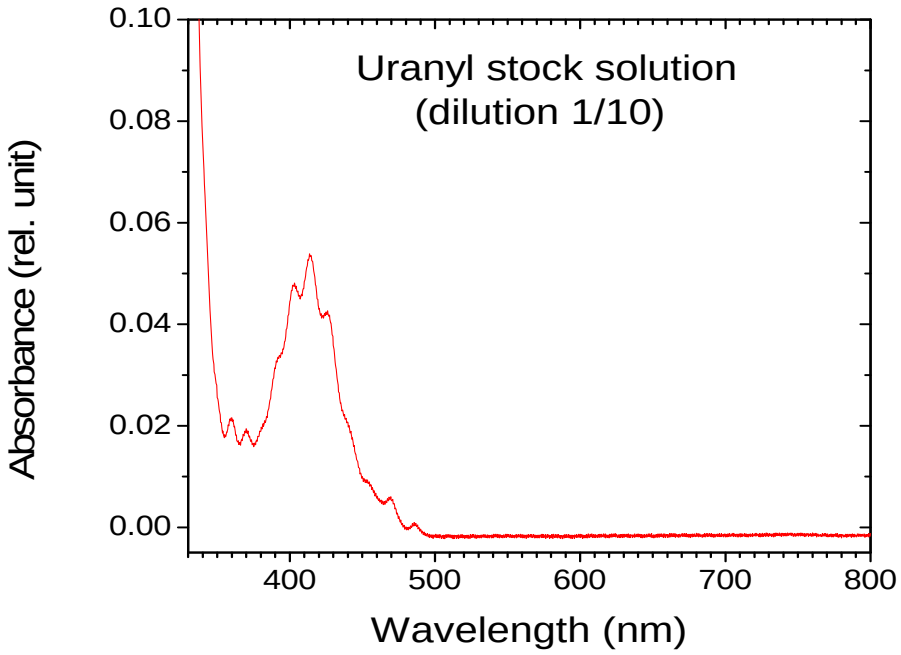

Figure 4-2. Absorption spectrum of the prepared uranyl stock solution diluted 1/10 (so [U] = 15 mM). The absence of spectral features above 500 nm confirmed that there was no significant amount of U(IV) present.

Preparation of uranium (VI) solids (Subtask 8)

Four different uranium solid phases were used in the experiments conducted in Subtask 8 (see section 4.1.3): uranium peroxide (UO_4), uranium trioxide (UO_3), uranium hydroxide ($UO_2(OH)_2$), and uranium precipitates obtained in brine from over-saturation in similar experimental conditions (same brine, about the same pC_{H+} value, etc.). These solids represent a range of likely precipitates in irradiated oxic to anoxic carbonate-free brine systems with U(VI). The first three uranium solids were synthetic uranium (VI) phases that could be formed in high radiation media (UO_4), or in potentially high oxidation media (UO_3), or in highly basic conditions ($UO_2(OH)_2$). The uranium precipitates were generated in the same experimental conditions described in the over-saturation experiments in carbonate-free brine reported in section 4.3.1 and more extensively in the LCO-ACP-10 report [Lucchini 2010a]. It should be noted that the uranium precipitates have not been fully characterized yet, so their structure and composition is unknown at this time. Some attempts of solid characterization have been made by XANES, XRD and SEM/EDS, and these results are reported in section 4.3.1.3.

These different uranium (VI) solids were all generated in the ACRSP laboratory, and a description of their preparation follows.

Uranium peroxide (UO_4)

Uranium peroxide was generated according to the following reaction [Brady 1948]:

$$UO_2^{2+} + H_2O_2 \Leftrightarrow UO_4 + 2H^+ \qquad K_{25°C} = 1.3\times10^{-3} \qquad 4\text{-}2$$

According to Cahill's work, uranium peroxide readily precipitates when uranyl ion is in the presence of an excess of hydrogen peroxide at pH < 5 [Cahill 1990].

A known amount of our uranyl stock solution was mixed with an excess of 30% hydrogen peroxide (H_2O_2) (ACS certified – Fisher) to readily generate a bright yellow precipitate of uranium peroxide. The precipitate was separated from the solution and recovered by centrifugation at room temperature. The uranium peroxide phase was confirmed using XRD analysis.

Uranium trioxide (UO_3)

It is well known that uranium peroxide loses an oxygen atom at 400°C [Katz 1986, p.267]. For our experiments, uranium peroxide was placed in an oven at 400°C for 5 hours, which led to a red coloration in the uranium solid that is characteristic of uranium trioxide. The uranium trioxide phase was confirmed using XRD analysis.

Uranium hydroxide ($UO_2(OH)_2$)

Uranium hydroxide precipitate was generated by adding a known concentration of our uranyl stock solution into an excess of low carbonate-content sodium hydroxide (50 weight% - ACS certified) in a nitrogen controlled atmosphere. The precipitate was recovered by centrifugation and dried in the same nitrogen controlled atmosphere.

Uranium precipitates

The uranium precipitates were generated under the same experimental conditions (same brine, about the same pC_{H+} value, etc.) described in the Subtask 1 over-saturation experiments in carbonate-free brine.

U(VI) solubility experiments

For the over-saturation approach (Subtasks 1 and 3), the U(VI) solubility experiments were initiated by the addition of uranyl spiked brine into the corresponding pC_{H+}-adjusted brine solutions, designated in the following experimental matrices: Table 4-1 for Subtask 1, and Table 4-2 for Subtask 3. For the under-saturation approach (Subtask 8), the U(VI) solubility experiments were initiated by the addition of a weighted amount of uranium solid phase into the corresponding pC_{H+}-adjusted brine solutions, designated in the experimental matrix (Table 4-3).

All of the experiments were carried out at (25 ± 4)°C in an anoxic carbon dioxide-free glovebox (MBraun Labmaster 130 with a nitrogen atmosphere and with an oxygen purification system).

Once underway, aliquots were periodically collected (0.3 mL) and filtered through Microcon® Millipore centrifugal filters (with a nominal molecular weight limit of 30,000 Daltons which corresponded to an approximate pore size of 10 nm) by centrifugation at 8000 or 13500 rpm for 13 or 15 minutes. The filtration step removed potential uranium colloids or particulates bigger than 10 nm from the sample aliquots.

Filtrates were analyzed for uranium content using an inductively coupled plasma mass spectrometer (ICP-MS) Elan model 6000 or Agilent 7500. Aliquots of the filtrates were diluted 50 or 100 times in dilute nitric acid due to the high salt concentration in the brines (i.e., to reduce matrix effects and salting out within the ICP-MS) and to establish uranium concentrations within the calibration range of the ICP-MS. The detection limit by ICP-MS for uranium was ~5×10^{-12} M, which translated to an effective concentration of ~2.5×10^{-10} M or ~5×10^{-10} M within the experiments, based on dilution factor.

4.2.2 Experimental Limitations and Considerations

There were a number of limitations and constraints on the experiments performed. The most important of these are described in this section. Some considerations to specific experimental aspects are also addressed.

Effect of pC_{H+} on brine stability

Both WIPP simulated brines, GWB and ERDA-6, contain significant concentrations of magnesium and calcium cations. At $pC_{H+} > 8.5$, these cations form insoluble hydroxide phases. The precipitation "cloud" point for each brine solution was established by titration with sodium hydroxide. Towards lower pC_{H+}, acid was added to operationally establish the buffering-range of the brine, i.e., the point at which pC_{H+} change is accelerated.

For titration with base, the cloud point observed was at $pC_{H+} \sim 8.7$ in GWB brine and at $pC_{H+} \sim 10.8$ in ERDA-6 brine. In acid titrations, the sharp decrease in pC_{H+} was observed at ~ 5.5 in both brines and corresponded to the end point of titration with borate, which is also a component of each simulated brine. A good correlation was found between the amount of acid added and the concentration of borate for each brine titrated.

The working pC_{H+} range was established between 6.0 and 8.7 for GWB brine, and between 7.0 and 10.8 for ERDA-6 brine (Figure 4-3).

For each brine, the higher pC_{H+} value corresponded to the "cloud" point where significant precipitation was observed. Above these values, the brine composition effectively changed. In our experimental matrix in carbonate-free brines (Table 4-1), the U(VI) solubility was investigated at pC_{H+} values above the respective cloud points.

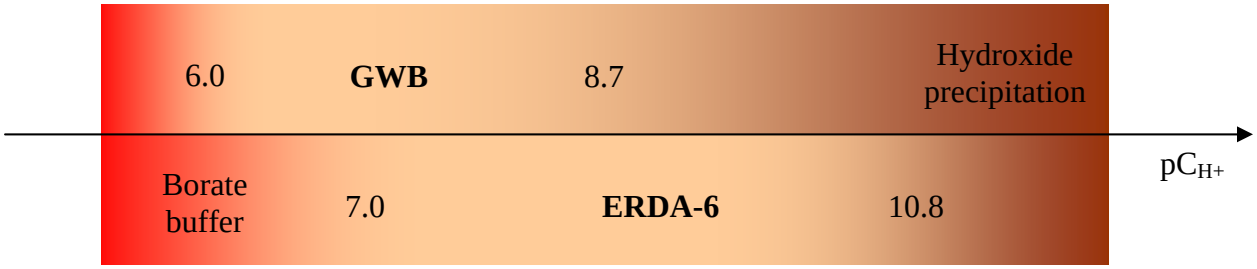

Figure 4-3. Chemical stability and working range of GWB and ERDA-6 brines versus pC_{H+}. The lower pC_{H+} value is defined by the buffering capacity and range of borate in the brines. The higher pC_{H+} value corresponds to the "cloud" point when precipitation occurs. The pC_{H+} boundaries have an accuracy of ± 0.5 pH unit.

Constant pC_{H+} values during the experiments performed in carbonate-free simulated brines (Subtask 1)

The stability of the pC_{H+} values in carbonate-free simulated brines over time was investigated using some experiments of Subtask 1. Before the second uranium spike addition, the pC_{H+} of all the experimental solutions of Subtask 1 was re-checked. After 214 days, no significant pC_{H+} drift (defined as < 0.3 pH units) from its initial value were observed. These pC_{H+} values were again checked after 369 days. As before, no significant shift was observed with the exception of the lowest selected pC_{H+} in ERDA-6. In this case, the initial pC_{H+} decreased from 6.9 to 6.2 after the second uranyl addition, despite the small volume of uranyl added to the solution (about 1% of the total volume). This occurred due to the acidity of the second uranyl addition in the brine since it was at the lower range of its buffer capacity. Despite these exceptions, our overall observation was that the high buffer capacities of the simulated WIPP brines led to high pC_{H+} stability. This was only true for the carbonate-free simulated WIPP brines ERDA-6 and GWB. In the presence of carbonate, the pC_{H+} values tend to drift. It was necessary to adjust the pC_{H+} during the experiments when carbonate was present (Subtask 3).

Potential effect of filtration

A potential experimental complexity was the effect of the Microcon® Millipore centrifugal filters (nominal molecular weight limit: 30,000 Daltons) used in this study on the measured uranium concentration. There was a possibility that the filter membrane selected for the experiments could retain uranium species smaller than 10nm by chemical affinity or adsorption, to result in lower measured concentrations compared to concentrations in the experiments. This potential effect was evaluated using some experiments in Subtask 1 to confirm our experimental approach.

Figure 4-4 displays the time profiles of uranium concentration in GWB brine at pC_{H+} = 6.3 and in ERDA-6 brine at pC_{H+} = 8.1 in a nitrogen controlled atmosphere and up to 369 days of experiments in Subtask 1. For each brine case, two time profiles are represented. In the first profile, the sampled aliquots were filtered through a 30 kDa filter. In the second profile, extra aliquots were sampled but not filtered. In general, difference between unfiltered and filtered data for the same brine and experimental conditions is generally within the calculated uncertainty of the data (see section 4.2.3) indicating that the 30 kDa filter membrane used in the experiments did not significantly retain (< 10%) uranium during the filtration of the aliquots.

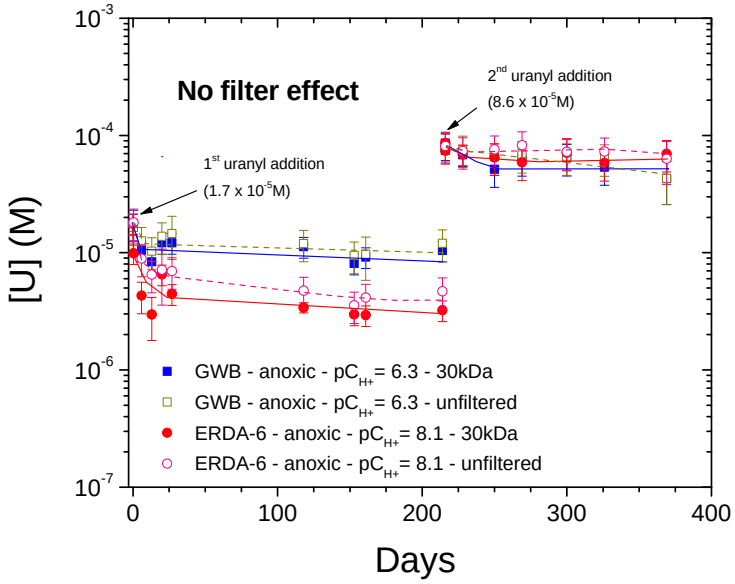

Figure 4-4. Time profiles of uranium concentration in GWB brine at pC_{H+}= 6.3 (square scatter) and in ERDA-6 brine at pC_{H+}= 8.1 (circle scatter) in the nitrogen controlled atmosphere and up to 369 days of Subtask 1 experiments. For each brine case, the sampled aliquots were filtered through a 30 kDa filter (filled scatter), and extra aliquots were sampled but not filtered (open scatter). The difference between unfiltered and filtered data for the same brine and experimental conditions is generally within the calculated uncertainty of the data. The 30 kDa filter used in the experiments did not exhibit any significant retention of uranium during the filtration of the aliquots.

Limitations in the detection of U using ICP-MS

The concentration of uranium in all of the solubility experiments was determined using ICP-MS Elan 6000 or Agilent 7500. An indium internal standard was used during the analyses to account for matrix and other effects. An acceptable indium recovery range of 60% to 120% was used. Each brine sample was diluted by a factor of 50 or 100 prior to ICP-MS analysis in order to alleviate instrument clogging, signal suppression, and other effects. A 0.5% nitric acid media was used for sample dilution. The nitric acid media was prepared

using high purity nitric acid (99.9999% purity, Alfa Aesar) and water (18 MΩ·cm). The ICP-MS response was calibrated using a suite of uranium calibration standards that had been prepared from a NIST-traceable stock solution (High Purity Standards) in 0.5% nitric acid to provide matrix matching. The approximate detection limit of the instrument for uranium under these conditions was 5×10^{-12} M. This led to an effective detection limit of ~5×10^{-10} M in the brines due to the necessary dilutions made in sample preparations, or in the few cases of a 50 times dilution, ~2.5×10^{-10} M.

4.2.3 Error Analysis

The measurement of uranium concentration was the main experimental goal in these solubility studies. There are a number of sources of error that could potentially contribute to the uncertainty in the uranium concentrations measured.

The most significant contribution to the uncertainty in the uranium concentration determination was the ICP-MS analysis, particularly when the concentrations measured approached the instrument detection limit. The estimated error on the uranium concentration measured by ICP-MS was approximately 100% at the working detection limit (5×10^{-10} M), about 70% at 10^{-8} M, and about 20% at 10^{-6} M uranium. The accuracy of the ICP-MS measurements was determined by the linear response of the instrument to a dilution series of seven (or eight depending on the sampling series) uranium standards in the concentration range of 5 ppb to 1000 ppb or 2000 ppb. Periodic continuing checks of the instrument calibration validity were performed and observed to be within 90 to 110% of the known value, indicating that the instrument remained in calibration throughout the analysis. Sample replicates versus measurement replicates were performed to confirm the precision of the ICP-MS measurements (Table 4-1 to Table 4-3).

The experimental error attributed to pipetting was approximately 1%. Due to the high ionic strength, each sample was diluted by a factor of 100; therefore, this operation contributed a total approximate error of 10% in the ICP-MS analysis.

The overall uncertainty, accounting for all sources of uncertainty described above, in the uranium concentration determination were evaluated to be about 20% at 10^{-5} M or higher, about 30% at 10^{-6} M, about 40% at 10^{-7} M, about 80% at 10^{-8} M, and 100% for uranium concentrations below 5×10^{-10} M.

It should be noted that the pC_{H+} measurements also had experimental error. The pC_{H+} was measured with an uncertainty of 0.1 pH unit. These errors in $pC_{H+,}$ although present, are not included in the graphs to preserve their clarity.

4.3 Results and Discussion

The results of our U(VI) solubility study are summarized and discussed in this section.

In section 4.3.1, we report the data from the experiments on U(VI) solubility in carbonate-free brines using the over-saturation approach (Subtask 1). These data were already presented and discussed in other publications [Lucchini 2010a, 2010b, 2013]. The results obtained in the under-saturation experiments (Subtask 8) are given in section 4.3.2. The results on the investigation of the effect of carbonate on U(VI) solubility are presented in section 4.3.3 (Subtask 3). Any significant changes in pC_{H+} measured in solution that occurred and were corrected are described in the text.

4.3.1 U(VI) solubility under anoxic conditions in carbonate-free brine (Subtask 1)

The results of our U(VI) solubility in carbonate-free brines study using the over-saturation approach for our Subtask 1 experimental matrix (Table 4-1) are summarized and discussed in this section.

The U(VI) concentration in carbonate-free GWB brine and ERDA-6 brine at different pC_{H+} are presented respectively in sections 4.3.1.1 and 4.3.1.2. These data correspond to a total of 19 samplings performed for each brine and pC_{H+} investigated in a nitrogen controlled atmosphere over 705 days.

These data led to the determination of the solubility of uranium (VI) in the range of pC_{H+} investigated. The resulting U(VI) solubility in carbonate-free GWB brine and in carbonate-free ERDA-6 brine is discussed in section 4.4, in the light of the data obtained in the experiments using the under-saturation approach (Subtask 8).

4.3.1.1 Evolution of U(VI) concentration with time in carbonate-free GWB brine

Figure 4-5 shows the uranium concentration data measured as a function of time and at four different pC_{H+} values in carbonate-free GWB brine that had been placed in nitrogen controlled atmosphere for the 705-day duration of the experiment.

The initial uranyl concentration was $(1.7 \pm 0.3)\times10^{-5}$ M. The data in Figure 4-5 show that steady-state uranium concentrations were rapidly achieved (i.e., in less than 20 days) in GWB brine. These concentrations were confirmed by the second uranium addition in all of the investigated pC_{H+} values with the exception of the lowest pC_{H+} (6.3). This second uranium addition was performed after 216 days of experiment, and was $(8.6 \pm 1.7)\times10^{-5}$ M, which was about 5 times the initial uranium spike. At $pC_{H+} = 6.3$, the steady-state uranium concentration established after the first uranyl addition was about 10^{-5} M, but this value was not re-established at the time of the last sampling (day 705), that is 489 days after the second uranyl addition in solution. For all the other investigated pC_{H+} values (≥ 7), steady-state uranium concentrations were re-established in about 50 days, so a somewhat slower equilibration time was noted.

The steady-state uranium concentration in solution depended on pC_{H+}, as expected. The concentration of uranium increased with lower pC_{H+}. The uranium concentration achieved a steady-state in carbonate-free GWB brines when it reached about 10^{-5} M at $pC_{H+} = 6.2$, and about 10^{-6} M at $pC_{H+} = 9.2$. At the investigated intermediate pC_{H+} values (7.4 and

8.2), the results didn't follow the expected trend on the graph (Figure 4-5): the uranium concentration at pC_{H+} = 7.4 was lower than the uranium concentration at pC_{H+} = 8.2. However, there was only a factor of two between the two concentrations: about 2×10^{-6} M at pC_{H+} = 7.4, and about 4×10^{-6} M at pC_{H+} = 8.2. This difference appears significant in Figure 4-5, due to the use of the semi-logarithm scale, but it is not actually significant.

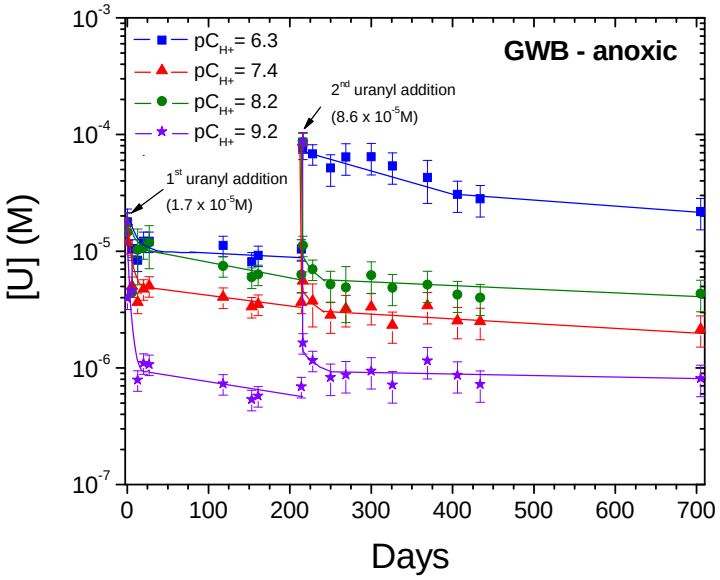

Figure 4-5. Uranium concentration in carbonate-free GWB brine in a nitrogen controlled atmosphere as a function of time. Time profiles correspond to pC_{H+} = 6.3, 7.4, 8.2 and 9.2 from top to bottom of the legend. These data correspond to 19 samplings performed over 705 days.

After the second uranium addition, yellow precipitates were observed in all GWB solutions at $pC_{H+} \geq 7$. These precipitates were presumably due to the formation of uranyl hydroxide phases, but characterization of the solids is ongoing. No precipitate was observed at the lowest pC_{H+} of 6.2. Also, the solution at pC_{H+} = 9.2 didn't exhibit any clearly visible precipitation from brine components before the second uranyl addition, even though this pC_{H+} value is beyond the stability domain of GWB (Figure 4-3).

4.3.1.2 Evolution of U(VI) concentration with time in carbonate-free ERDA-6 brine

The uranium concentration data measured as a function of time and five different pC_{H+} values in carbonate-free ERDA-6 brine that had been placed in a nitrogen controlled atmosphere for the 705-day duration of the experiment are shown on Figure 4-6.

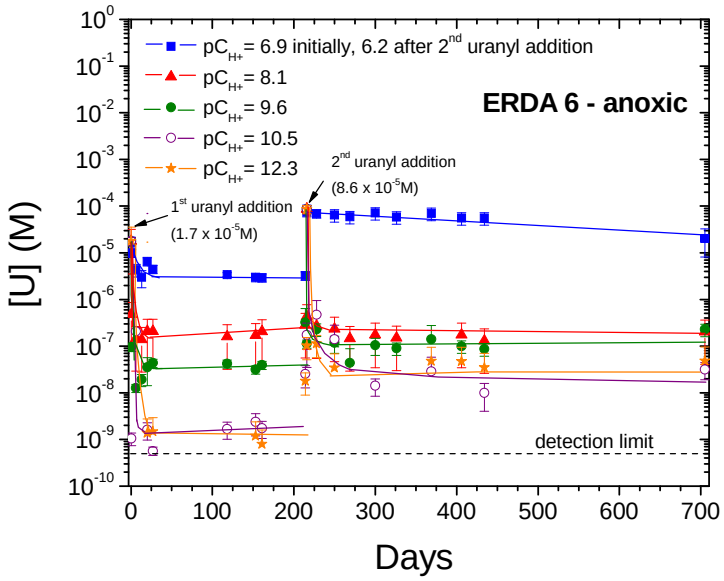

Figure 4-6. Uranium concentration in carbonate-free ERDA-6 brine in a nitrogen controlled atmosphere as a function of time. Data shown are for pC_{H+} = 6.2 (initially 6.9), 8.1, 9.6, 10.5 and 12.3 from top to bottom of the legend. These data correspond to 19 samplings performed over 705 days.

The initial uranyl concentration in the ERDA-6 brine experiments was $(1.7\pm0.3)\times10^{-5}$ M. This was approximately the expected solubility of uranium in ERDA-6 brine as established in our developmental experiments. Similar to the experiments in GWB, a second uranyl spike was added to every solution at day 216 to re-establish over-saturation with respect to uranium concentration. This second uranium addition was $(8.6 \pm1.7)\times10^{-5}$ M, which was about 5 times the initial uranium spike. As with GWB, the later uranium additions had a somewhat slower equilibration time. It took about 20 days to reach steady-state after the initial uranyl spike addition, and about 50 days after the second uranyl addition. These rates in ERDA-6 were similar to the rates obtained in GWB.

The uranium steady-state concentrations were not all reproducible after the first and the second uranyl addition. Only at pC_{H+} = 8.1 and, to some extent at pC_{H+} = 9.6, the steady-state uranium concentrations were the same after the first and after the second uranyl additions. At pC_{H+} = 8.1, the uranium concentration found in solution was about 2×10^{-7} M, regardless of the uranium addition. At pC_{H+} = 9.6, the steady-state uranium concentration was about 1×10^{-7} M after the second uranyl addition, which is only two times more than the concentration established before the second uranyl addition.

Discrepancies in the steady-state uranium concentrations were noticed for the lowest pC_{H+} values and the two highest pC_{H+} values investigated. At the lowest pC_{H+} value, the addition of uranium stock led to a decrease in pC_{H+} from 6.9 to 6.2 leading to an order of magnitude increase in the measured steady-state uranium concentration (2×10^{-6} M to 2 x 10^{-5} M).

The two highest pC_{H+} brines investigated (10.5 and 12.3) showed an order of magnitude increase in the steady-state uranium concentrations obtained before and after the second uranyl addition (~10^{-9} M to ~2×10^{-8} M).There was no change in the pC_{H+} measured after the second uranyl addition so the cause of this change in steady-state concentration is not clear yet. Yellow precipitates were generated in all ERDA-6 solutions at $pC_{H+} \geq 8$ a few days after the second uranyl addition. These were initially uranium hydroxide phases that may have gone through phase transformations over time. For example, the precipitate observed at pC_{H+} = 10.5 turned from yellow to white about 40 days after the addition of the second uranyl spike [Lucchini 2010b].

4.3.1.3 Solids characterization of uranium precipitates

An attempt to characterize the solids formed in these Subtask 1 uranium (VI) solubility experiments was made. X-ray Absorption Near Edge Spectroscopy (XANES) analysis was performed at the Argonne Advanced Photon Source on the precipitates from the following three samples: ERDA-6 at pC_{H+} = 12.3, ERDA-6 at pC_{H+} = 10.5, and GWB at pC_{H+} = 9.3. Three uranium (VI) solids prepared in our laboratory (see section 4.2.1) were also analyzed as references. The XANES spectra of these five solid samples taken at the uranium L_3 thresholds are shown in Figure 4-7. These results confirm the uranium oxidation state to be U(VI) but did not permit EXAFS due to the high disorder in the samples – presumably due to the amorphous nature and the likely presence of several phases in the precipitates.

Some solid characterization was also carried out by Scanning Electron Microscopy (SEM) using a Hitachi model S-3400N Type II scanning electron microscope equipped with an Energy-Dispersive x-ray Spectrometer (EDS - Thermo Electron NORAN System Six 300). Figure 4-8 shows SEM images of the precipitate obtained in ERDA-6 solution at pC_{H+}=10.5. The presence of uranium in the bright “white” aggregates on the SEM image could be detected by EDS but we could not identify the phase present. These uranium aggregates were found among other solid phases containing mostly sodium, magnesium, oxygen and chloride (brine-related phases) although the samples were washed [Lucchini 2013].

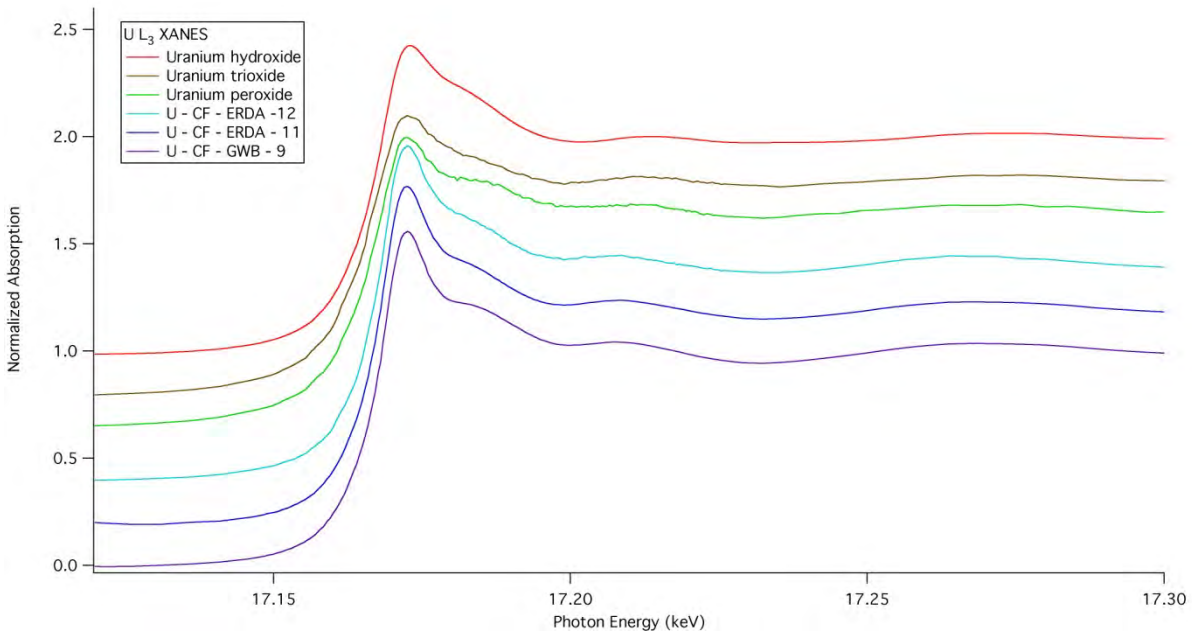

Figure 4-7. XANES spectra of five uranium solid samples taken at the uranium L_3 thresholds. From the top to the bottom, the spectra are from the following solid samples: uranium hydroxide, uranium trioxide, uranium peroxide, ERDA-6 at pC_{H+} = 12.3, ERDA-6 at pC_{H+} = 10.5 and GWB at pC_{H+} = 9.3.

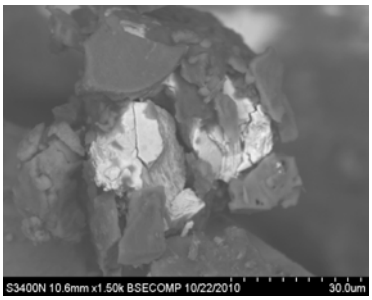

Figure 4-8. Scanning Electron Microscopy image of the precipitates obtained in ERDA-6 solution at pC_{H+}=10.5 (magnification: 1500×). The bright white solids were the uranium phases. The surrounding solids were composed of sodium, magnesium, oxygen and chloride [Lucchini 2013].

4.3.2 U(VI) solubility in brine from under saturation (Subtask 8)

In Subtask 8, uranium (VI) solubility experiments were conducted in carbonate-free ERDA-6 and GWB brines using the under-saturation approach. The experimental matrix was given in Table 4-3. Four different uranium solid phases were used: uranium peroxide (UO_4), uranium trioxide (UO_3), uranium hydroxide ($UO_2(OH)_2$), and uranium precipitates obtained in ERDA-6 brine using the over-saturation approach and in similar experimental conditions (same brine, about the same pC_{H+} value, etc.). The preparation of these uranium solids is described in section 4.2.1.

The experimental data obtained in this Subtask 8 are presented herein. The evolution of uranium concentration with time in GWB brine and ERDA-6 brine is shown in section 4.3.2.1 and 4.3.2.2 respectively.

4.3.2.1 Evolution of U(VI) concentration with time in carbonate-free GWB brine in the under-saturation experiments

A pre-determined amount of each of these four different uranium solid phases was added to carbonate-free GWB solutions, at four different pC_{H+} values: 6.3, 7.4, 8.2 and 9.3. The amount of uranium released into solution was monitored over time, using ICP-MS. For the four different uranium solid phases investigated, the time profile of the uranium concentration measured in solution was plotted as a function of the four different pC_{H+} values investigated.

Figure 4-9, Figure 4-10, Figure 4-11 and Figure 4-12 show uranium concentration data obtained at the four different pC_{H+} values investigated, from the experiments with respectively uranium peroxide (Figure 4-9), uranium trioxide (Figure 4-10), uranium hydroxide (Figure 4-11), and uranium precipitates obtained in over-saturation experiments (Figure 4-12). These data correspond to 9 samplings performed over a period of 1037 days (almost three years) of experiments. The total amount of uranium added in solution as a solid (i.e., the maximum concentration of uranium possible in solution) is also plotted in these Figures using a dashed line. The values were calculated using the minimum mass of precipitate added in solution (this was measured experimentally), the estimated formula weight of the precipitate, and the volume of solution. Attaining this calculated uranium concentration would mean that the uranium solid added to the solution was fully dissolved.

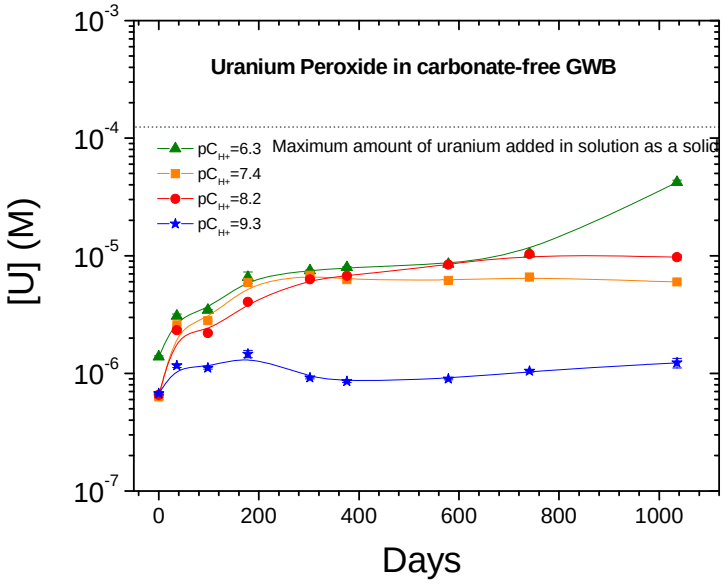

Figure 4-9. Evolution of uranium concentration in carbonate-free GWB solutions in the presence of solid uranium peroxide, with time at different pC_{H+} values, in nitrogen controlled atmosphere. The horizontal dotted line (….) represents the maximum uranium concentration if the entire solid added goes into solution. These data correspond to 9 samplings performed over 1037 days (under-saturation approach).

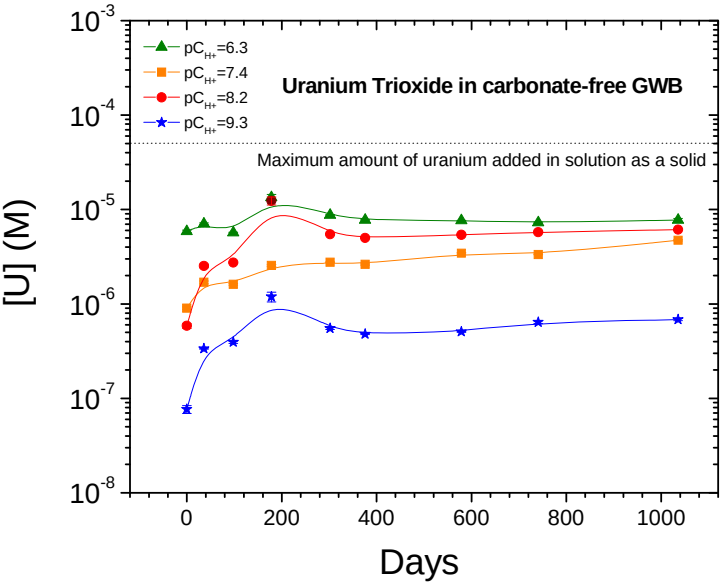

Figure 4-10. Evolution of uranium concentration in carbonate-free GWB solutions in the presence of solid uranium trioxide, with time at different pC_{H+} values, in nitrogen controlled atmosphere. The horizontal dotted line (….) represents the maximum uranium concentration if the entire solid added goes into solution. These data correspond to 9 samplings performed over 1037 days (under-saturation approach).

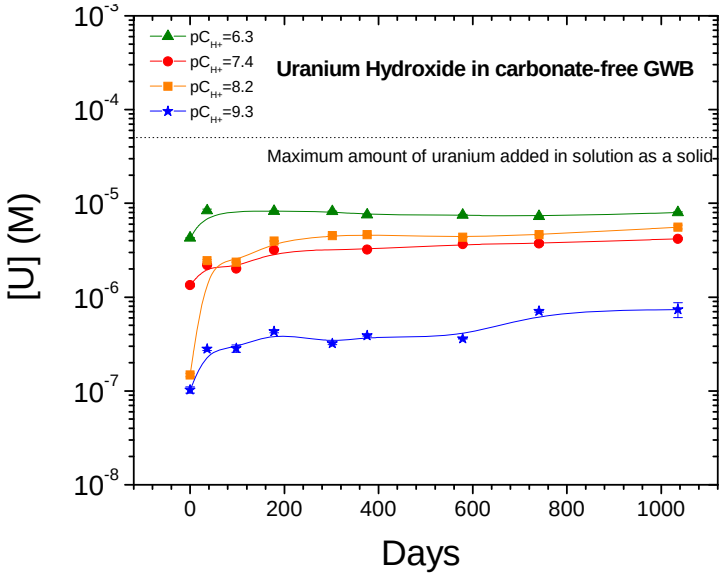

Figure 4-11. Evolution of uranium concentration in carbonate-free GWB solutions in the presence of solid uranium hydroxide, with time at different pC_{H+} values, in nitrogen controlled atmosphere. The horizontal dotted line (….) represents the maximum uranium concentration if the entire solid added goes into solution. These data correspond to 9 samplings performed over 1037 days (under-saturation approach).

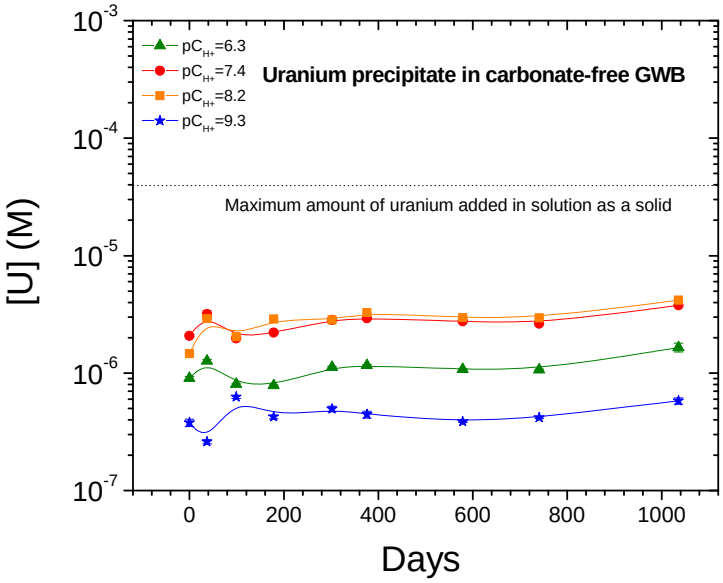

Figure 4-12. Evolution of uranium concentration in carbonate-free GWB solutions in the presence of solid uranium precipitate obtained in over-saturation experiments, with time at different pC_{H+} values, in nitrogen controlled atmosphere. The horizontal dotted line (….) represents the maximum uranium concentration if the entire solid added goes into solution. These data correspond to 9 samplings performed over 1037 days (under-saturation approach).

A few observations could be made from these data:

a) Steady-state conditions were reached in most of the experiments.

Steady-state uranium concentrations were achieved after ~ 400 days of the experiments in all solutions except one. The uranium concentrations measured after that time were almost unchanged for each case scenario of pC_{H+} value and uranium phase investigated, except one. The only exception would be for the data related to the uranium peroxide experiment at $pC_{H+} = 6.3$ (Figure 4-9): the last data point at day 1037 is higher than the previous data points and a steady increase in concentration was noted.

In addition to the stable concentrations of uranium measured in solution after ~ 400 days of the experiments, all the uranium solids initially placed in solution were still visible throughout the 1037 days of experiments. On each graph, a horizontal dotted line shows the maximum amount of uranium (converted to mole/L unit) that was initially placed into solution as a solid phase. For all experimental conditions, this line was not approached by any uranium concentration data measured in solution. In other words, the uranium concentrations measured in solution were well below the maximum concentration of uranium available to be released in solution (i.e. if the entire solid would be dissolved) after 1037 days of the experiments.

b) Concentrations of uranium released in solution were the lowest at $pC_{H+} = 9.3$.

The uranium concentrations measured in solution were consistently higher at $pC_{H+} < 9.3$, whatever uranium solid was used. In these conditions of pC_{H+}, they were in the range of 5×10^{-6} to 10^{-5} M in the experiments with the synthetic uranium solid phases (peroxide, trioxide, hydroxide), and in the range of 10^{-6} to 7×10^{-5} M in the experiments performed with the uranium precipitates. At $pC_{H+} = 9.3$, the uranium concentrations measured in solution were about or below 10^{-6} M. These lower uranium concentrations were accompanied by a white precipitate which occurred very early in the experiments (after 30 days). As a reminder, at $pC_{H+} = 9.3$, GWB brine is chemically unstable, and a white precipitate (most likely magnesium hydroxide) is present in solution (see Table 4-3).

c) Data in these under-saturation experiments were in good agreement with the data obtained in the over-saturation experiments.

The observed solubility for these under-saturation experiments with uranium precipitates was about 10^{-6} M at $6.3 \leq pC_{H+} \leq 9.3$ (see Figure 4-12). A similar result was observed in the over-saturation experiments in carbonate-free GWB (see section 4.3.1.1).

4.3.2.2 Evolution of U(VI) concentration as a function of time in carbonate-free ERDA-6 brine in the under-saturation experiments

A pre-determined amount of each of four different uranium solid phases was added to carbonate-free ERDA-6 solutions, at five different pC_{H+} values: 7.0, 8.2, 9.6, 10.5 and 12.5. The amount of uranium released into solution was monitored over time using ICP-MS. The time profile of the uranium concentration measured in solution was plotted as a function of pC_{H+} and uranium solid phase used.

Figure 4-13, Figure 4-14, Figure 4-15, and Figure 4-16 show uranium concentration data obtained at the five different pC_{H+} values investigated, from the experiments with uranium peroxide (Figure 4-13), uranium trioxide (Figure 4-14), uranium hydroxide (Figure 4-15), and uranium precipitates obtained in over-saturation experiments (Figure 4-16). These data correspond to 9 samplings of the experiments performed over 1037 days (almost three years). Similar to the experiments conducted in GWB, the maximum amount of uranium added in solution as a solid is also plotted in these Figures using a dashed line. The values were calculated using the minimum mass of precipitate added in solution (this was measured experimentally), the estimated formula weight of the precipitate, and the volume of solution. Attaining this calculated uranium concentration would mean that the uranium solid added to the solution was fully dissolved.

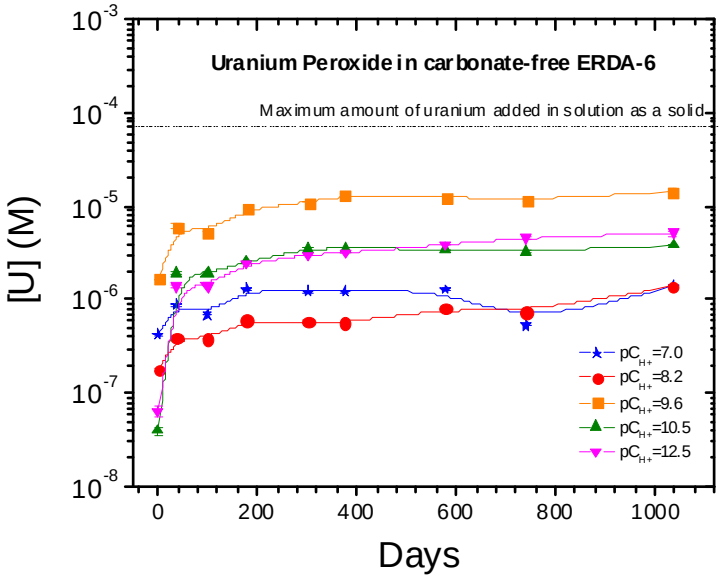

Figure 4-13. Evolution of uranium concentration in carbonate-free ERDA-6 solutions in the presence of solid uranium peroxide, with time at different pC_{H+} values, in nitrogen controlled atmosphere. The horizontal dotted line (…...) represents the maximum uranium concentration possible if the entire solid added goes into solution. These data correspond to 9 samplings performed over 1037 days (under-saturation approach).

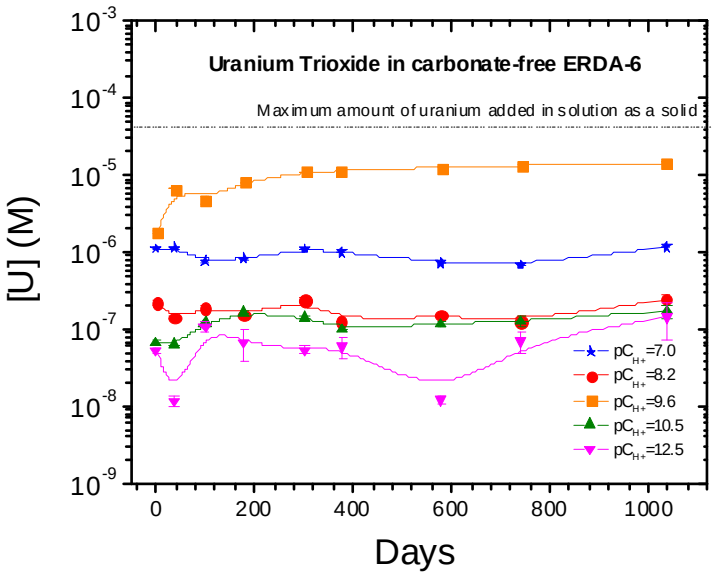

Figure 4-14. Evolution of uranium concentration in carbonate-free ERDA-6 solutions in the presence of solid uranium trioxide, with time at different pC_{H+} values, in nitrogen controlled atmosphere. The horizontal dotted line (…...) represents the maximum uranium concentration if the entire solid added goes into solution. These data correspond to 9 samplings performed over 1037 days (under-saturation approach).

A few observations could be made from these data:

a) Steady-state conditions were apparent in most of the experiments.

The following three observations indicated that steady-state uranium concentrations in solution could be achieved in all of the experiments.

First, in all of the experiments, the uranium concentrations measured after 1037 days of the experiments were well below the concentrations expected if the entire uranium solid had dissolved.

Second, for each experiment, the uranium concentrations measured were virtually unchanged over time after ~ 400 days (or earlier in some cases).

Third, the uranium oxides (i.e., peroxide, trioxide, and hydroxide), initially introduced as solids, were still visually observed in all solutions. On each graph (Figure 4-13 through Figure 4-16), a horizontal dotted line shows the maximum amount of uranium (converted to mole/L unit) that was initially placed into solution as a solid phase. In all experimental conditions, this line was not approached by any uranium concentration data measured. The uranium concentrations measured in solution were well below the maximum

concentration of uranium available for potential release in solutions (i.e. if the entire solid would be dissolved) after 1037 days of the experiments. An exception to this was with the uranium precipitates, which could not be visually seen any more in ERDA-6 solutions at $pC_{H+} < 11$. However, in this case, since the uranium measured in solution was also below what was expected if the entire uranium solid had dissolved, we suspect that the uranium solid initially introduced in solution had broken into invisible fragments over time. The other possible explanation could have been that the uranium solid initially introduced in solution completely dissolved, generating a uranium concentration of about 10^{-7} M. However, the mass of the initial uranium solid would have been a few micrograms, which would have been impossible to measure with our balances.

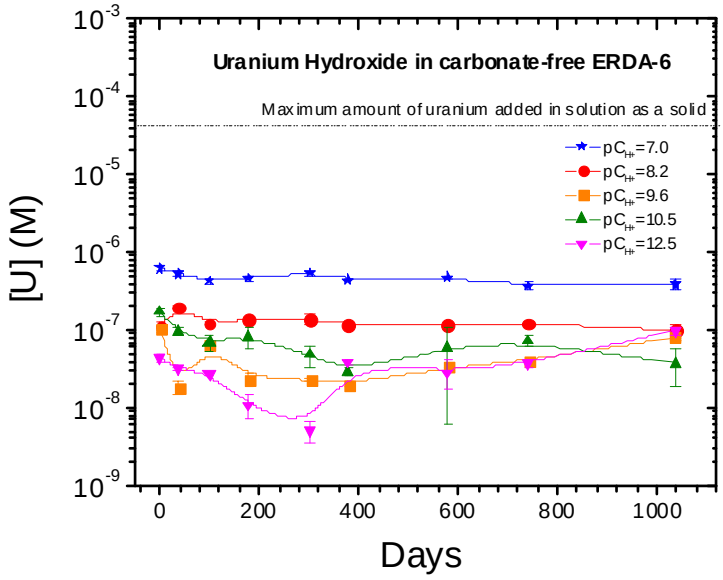

Figure 4-15. Evolution of uranium concentration in carbonate-free GWB solutions in the presence of solid uranium hydroxide, with time at different pC_{H+} values, in nitrogen controlled atmosphere. The horizontal dotted line (…...) represents the maximum uranium concentration possible if the entire solid added goes into solution. These data correspond to 9 samplings performed over 1037 days (under-saturation approach).

b) Concentrations of uranium released in solution were approximately 10^{-5} M or lower.

The uranium concentrations measured in solution were approximately 10^{-5} M or lower at all pC_{H+} conditions investigated, i.e., pC_{H+} 8.2 to 12.5, regardless of the uranium source. Concentrations ranged from 10^{-7} to 10^{-5} M in the experiments with the uranium peroxide and trioxide, and from 3×10^{-8} to 3×10^{-6} M in the experiments performed with the

uranium precipitates and hydroxide. At the two highest pC_{H+} investigated (i.e., pC_{H+}10.5 and 12.5), the uranium concentrations measured in solution were about or below 10^{-7} M, with the exception of the experiments performed with uranium peroxide (10^{-7} – 10^{-5} M). In addition to lower uranium concentrations at pC_{H+} 10.5 and 12.5, a white precipitate was also observed to have formed very early in the experiments (after 30 days). As a reminder, the chemical stability of ERDA-6 brine is in the range $(7.0 \pm 0.5) \leq pC_{H+} \leq (10.8 \pm 0.5)$ (see Table 4-3). The two highest pC_{H+} investigated (i.e., pC_{H+} 10.5 and 12.5) in these Subtask 8 experiments were beyond this range, and therefore, a white precipitate, most likely magnesium hydroxide, was not unexpected in solution.

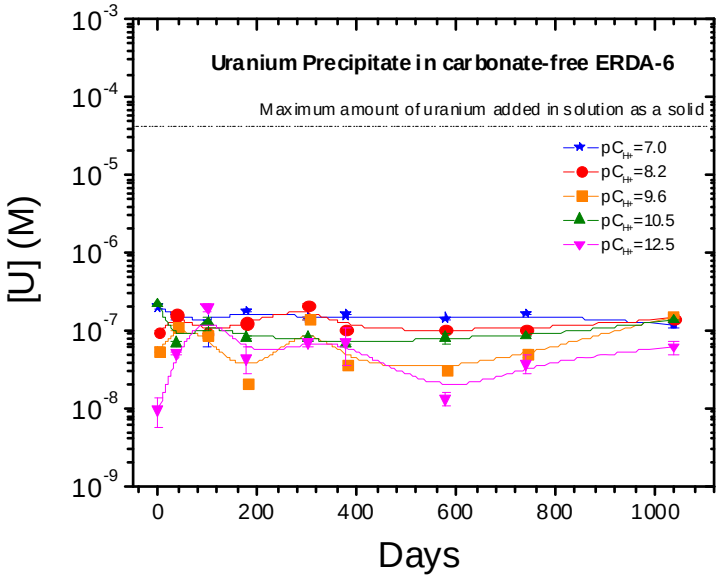

Figure 4-16. Evolution of uranium concentration in carbonate-free GWB solutions in the presence of solid uranium precipitate obtained in over-saturation experiments, with time at different pC_{H+} values, in nitrogen controlled atmosphere. The horizontal dotted line (…...) represents the maximum uranium concentration possible if the entire solid added goes into solution. These data correspond to 9 samplings performed over 1037 days (under-saturation approach).

c) Data in the present under-saturation experiments were in good agreement with the data obtained in the over-saturation experiments.

The data obtained with uranium precipitates (see Figure 4-16) in these under-saturation experiments were about 10^{-7} M at all investigated pC_{H+} conditions (i.e., pC_{H+} 7.0 to 12.5). Similar results were obtained for the over-saturation experiments at pC_{H+} higher than 8 (see section 4.3.1.2).

4.3.3 Carbonate effects study on U(VI) solubility (Subtask 3)

The effect of carbonate on the solubility of uranium (VI) was investigated in Subtask 3. Experiments were performed in simulated WIPP brines, GWB and ERDA-6, and involved three different initial concentrations of carbonate in the solutions (i.e., no carbonate, 2×10^{-3} M, and 2×10^{-4} M) at two different pC_{H+} values. These experiments were initiated when uranyl ion, at a concentration of 1.48×10^{-5} M, was added to each of the solutions. A second uranyl-spike addition (1.0×10^{-4} M) was performed at day 231, and a third uranyl-spike addition (1.2×10^{-3} M) was done at day 675. The solutions were kept in sealed polypropylene bottles in a nitrogen controlled atmosphere throughout the experiment. Eighteen samples were taken over a 1073 day period for uranium analysis.

Experimental data obtained in GWB and ERDA-6 brines are presented herein, in sections 4.3.3.1 and 4.3.3.2 respectively. The pC_{H+} value of some solutions had to be slightly re-adjusted over time. If the changes were significant, they are mentioned in the text.

4.3.3.1 Evolution of U(VI) concentration as a function of time in GWB brine in the presence of carbonate

The uranium concentration data measured as a function of time in GWB at $pC_{H+} \sim 7.5$ and $pC_{H+} = 9$ in the absence or presence of two different initial concentrations of carbonate (2×10^{-4} M and 2×10^{-3} M) over the 1073 days of experiments are shown in Figure 4-17 and Figure 4-18, respectively.

In GWB at $pC_{H+} \sim 7.5$ (Figure 4-17), steady-state uranium concentrations were rapidly achieved (i.e., less than 20 days) at the start of the experiments. However, after the second addition of uranyl in the experimental solutions, the equilibration time was much longer (i.e., about 120 days), especially for the solutions with high carbonate content. After the third and final addition of uranyl, steady-state uranium concentrations were re-established very quickly, in a few days.

We observed that solid precipitation occurred in all the GWB solutions after the second uranyl-spike addition. Both the slow decrease of uranium in solution and the formation of yellow precipitates indicated that uranium precipitates were generated over time. We noticed that the precipitates got thicker after the third uranyl-spike addition, but the time to reach steady-state concentration of uranium in the solution was much shorter. Ultimately, we observed that the steady-state uranium concentrations (i.e., $\sim 2 \times 10^{-6}$ M) approached those obtained in the analogous carbonate-free GWB brine systems investigated, as described in section 4.3.1.1.

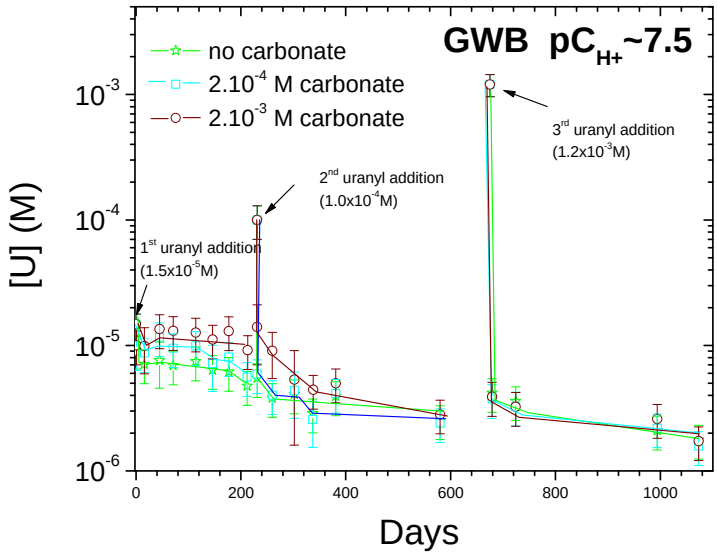

Figure 4-17. Uranium concentration in GWB as a function of time, at pC_{H+} ~ 7.5, in nitrogen controlled atmosphere, in the absence of carbonate or in the presence of two concentrations of carbonate (i.e., 2×10^{-4} M and 2×10^{-3} M) at the beginning of the experiments. These data correspond to 18 samplings performed over 1073 days.

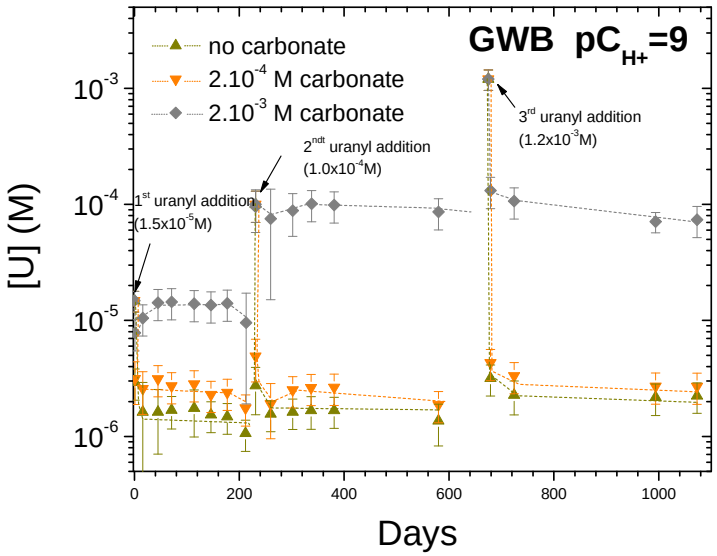

Figure 4-18. Uranium concentration in GWB as a function of time, at pC_{H+} = 9, in nitrogen controlled atmosphere, in the absence of carbonate or in the presence of two concentrations of carbonate (i.e., 2×10^{-4} M and 2×10^{-3} M) at the beginning of the experiments. These data correspond to 18 samplings performed over 1073 days.

At pC_{H+} = 9 in GWB solutions, however, (Figure 4-18), steady-state concentrations of uranium were systematically and rapidly achieved after each addition of uranyl-spike solution. In all solutions, we observed a bright yellow precipitate after the second uranyl-spike addition. The precipitates were thicker after the third uranyl-spike addition. Moreover, the concentrations of uranium measured in the solutions were reproducible. This indicated that steady-state concentrations of uranium were achieved in all of the solutions in these experiments at pC_{H+} = 9 using the over-saturation approach.

A significant impact of carbonate on uranium solubility was observed at the highest initial concentration of carbonate (i.e., 2×10^{-3} M) that was investigated. The uranium solubility in that case was about 10^{-4} M, which was two orders of magnitude higher than the uranium solubility values at no or low carbonate.

Similar to the pC_{H+} ~ 7.5 case, there was excellent agreement between the data obtained here (Subtask 3) in carbonate-free GWB at pC_{H+} = 9 and the data obtained under similar conditions in Subtask 1 (see section 4.3.1.1): a concentration of about 10^{-6} M was found in the two experiments.

4.3.3.2 Evolution of U(VI) concentration as a function of time in ERDA-6 brine in the presence of carbonate

In Figure 4-19 and Figure 4-20, we show the uranium concentration data measured as a function of time in ERDA-6 at pC_{H+} ~ 8.7 and pC_{H+} ~ 12 in the absence or presence of two different initial concentrations of carbonate (i.e., 2×10^{-4} M and 2×10^{-3} M) throughout the 1073 days of experiments.

In carbonate-free ERDA-6 at pC_{H+} ~ 8.7 (Figure 4-19), measured concentration of uranium was steady after each uranyl-spike addition. In addition, a yellow precipitate was formed after the second uranyl-spike addition, and got thicker after the third uranyl-spike addition. Consequently, we concluded that a steady-state uranium concentration of about 2×10^{-7} M was obtained at pC_{H+} ~ 8.7 in carbonate-free ERDA-6 brine. These results are in agreement with the experimental value obtained in Subtask 1 for the same system.

When carbonate was initially present in ERDA-6 at pC_{H+} ~ 8.7, the concentration of uranium in solution was still changing with time, even though the pC_{H+} values remained approximately constant. Despite the formation of a yellow precipitate in solution after the second uranyl-spike addition, it appeared that uranium steady-state concentrations were not yet achieved even after 1073 days of experiments. There is, however, a significant effect of carbonate on the concentration of uranium (Figure 4-19). Observed uranium concentrations for an initial concentration of 2×10^{-3} M carbonate, were approximately 2×10^{-5} M at day 1073. Only shortly after the third uranyl-spike addition (1.2×10^{-3} M at day 675), the uranium concentration measured in solution became saturated leading to precipitation. At that time, the maximum concentration of uranium measured in solution was about 2×10^{-4} M at days 679 and 724. The uranium concentrations showed a slow, but steady decrease with time after the third spike addition.

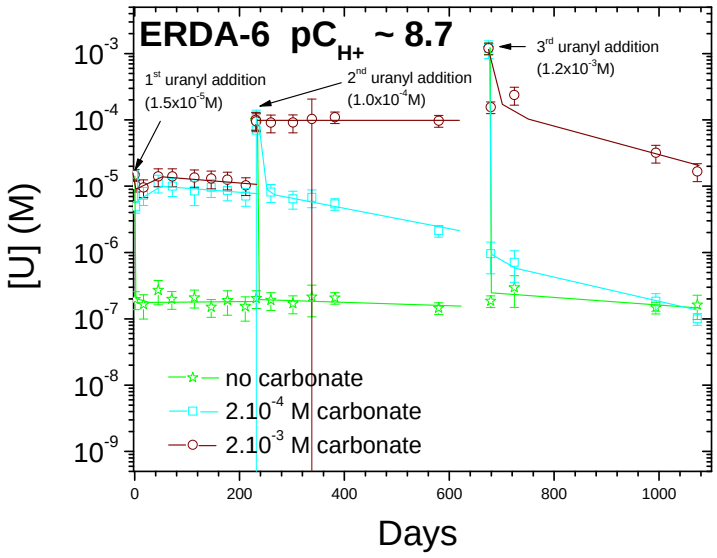

Figure 4-19. Uranium concentration in ERDA-6 as a function of time, at pC_{H+} ~ 8.7, in nitrogen controlled atmosphere, in the absence of carbonate or in the presence of two concentrations of carbonate (i.e., 2×10^{-4} M and 2×10^{-3} M) at the beginning of the experiments. These data correspond to 18 samplings performed over 1073 days.

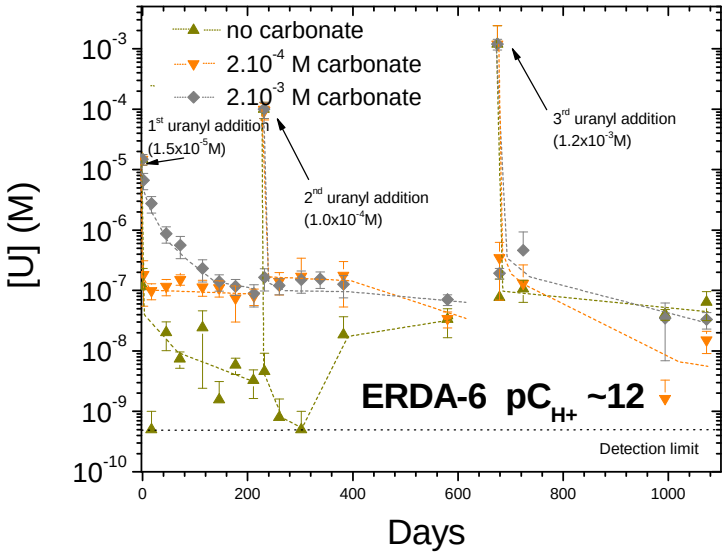

Figure 4-20. Uranium concentration in ERDA-6 as a function of time, at pC_{H+} ~ 12, in nitrogen controlled atmosphere, in the absence of carbonate or in the presence of two concentrations of carbonate (i.e., 2×10^{-4} M and 2×10^{-3} M) at the beginning of the experiments. These data correspond to 18 samplings performed over 1073 days.

The data presented for ERDA-6 at $pC_{H+} \sim 12$ (Figure 4-20) were obtained in a chemically heterogeneous system, since ERDA-6 brine exhibits precipitation beyond $pC_{H+} \sim 10.5$ (see section 4.2.2). A white precipitate was observed in all of the solutions a few days after the beginning of the experiments. The formation of a yellow precipitate at the bottom of the bottle was noticed after the second uranyl-spike addition in the carbonate-free and low carbonate content solutions. This precipitate was only visible in the high carbonate content experiments after the third uranyl-spike addition.

Steady-state concentrations of uranium in the ERDA-6 solutions at $pC_{H+} \sim 12$ were still not achieved by the last day of sampling (day 1073), despite the presence of a yellow precipitate (characteristic of a uranyl precipitate) in all of the solutions. At that time (day 1073), the uranium concentrations measured in solution, in the presence or the absence of carbonate, were between 10^{-8} M and 10^{-7} M. They were in this range of values prior to the third uranyl-spike addition, and after a two-unit pH adjustment was performed at days 382 and 580 of the experiments. Prior to the pH adjustment, the uranium concentrations measured in the solutions that initially contained carbonate were consistently about 10^{-7} M, even after the second uranyl-spike addition. This level of concentration was reached in less than 20 days in the low carbonate-content solution, but it took more than 120 days in the high carbonate-content solution for the uranium concentration to stabilize at this level.

Concerning the carbonate-free system, the results obtained in this Subtask are in good agreement with the results obtained in Subtask 1 (see section 4.3.1.2). A uranium concentration of about 10^{-7} M was measured in carbonate-free ERDA-6 at $pC_{H+} \sim 12$ in both experiments.

4.4 Solubility of U(VI) in the Absence of Carbonate

The evolution of uranium (VI) concentration with time in carbonate-free brines was presented in section 4.3.1 for the over-saturation approach, and in section 4.3.2 for the under-saturation approach. These data led to the determination of the solubility of uranium (VI) in carbonate-free WIPP simulated brines the range of pC_{H+} investigated. The results are discussed herein, and compared with published literature. The results presented in this section are for the final measured pC_{H+}, unless otherwise noted.

The overall uranium (VI) solubility measured in GWB and ERDA-6 brines in the absence of carbonate and in a nitrogen controlled atmosphere is plotted in Figure 4-21 as a function of pC_{H+}. This plot is based on the average of the time-dependent experimental data given in sections 4.3.1 (over-saturation) and 4.3.2 (under-saturation). In the over-saturation ERDA-6 experiments, the uranium concentration reached a steady-state over time, and precipitation occurred in the solutions at $pC_{H+} \geq 8$ (see section 4.3.1.2). In the under-saturation experiments, at $pC_{H+} < 11$, the solubility limit of uranium was reached (see section 4.3.2.2). Therefore, only the data obtained in ERDA-6 at $8 \leq pC_{H+} < 11$ in Figure 4-21 correspond to the true U(VI) solubility in the investigated systems.

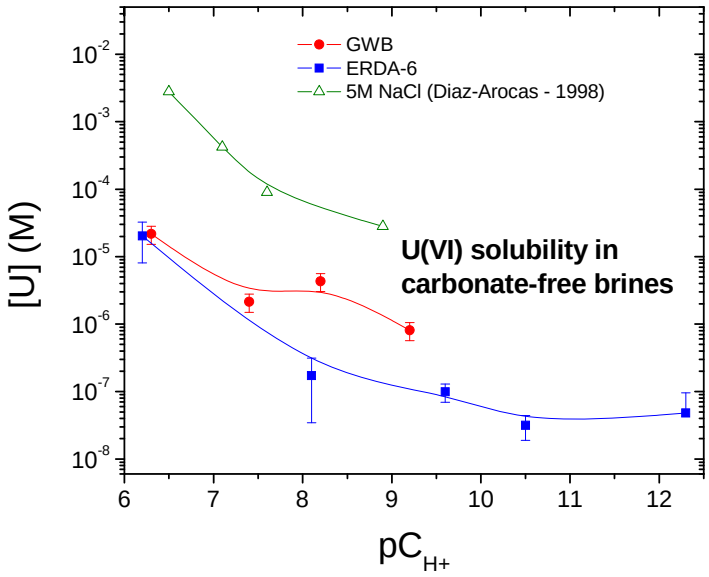

Figure 4-21. Uranium (VI) solubility in carbonate-free brines versus pC_{H+}. The two curves at the bottom of the graph are the average data obtained from our solubility experiments in GWB (curve in the middle of the graph) and in ERDA-6 (curve at the bottom of the graph) using the over-saturation approach and the under-saturation approach (polynomial fit). The top curve is based on the Diaz-Arocas' data in 5 M NaCl [Diaz-Arocas 1998].

The measured uranium solubilities were about 10^{-6} M (between 8×10^{-7} M and 5×10^{-6} M) in GWB brine at $pC_{H+} \geq 7$ and about 10^{-8} - 10^{-7} M (specifically between 3.1×10^{-8} M and 2.3×10^{-7} M) in ERDA-6 at $pC_{H+} \geq 8$. The uranium solubility decreased slightly from pC_{H+} ~ 8 to pC_{H+} ~ 11. At pC_{H+} ~ 12.3, which is beyond the chemical stability of ERDA-6, the solubility of uranium (VI) in carbonate-free solution was ~4.8×10^{-8} M.

These results definitively put an upper bound of ~ 10^{-5} M for the solubility of uranyl in the carbonate-free WIPP brines under the investigated range of experimental conditions ($pC_{H+} \geq 7$). At the expected pC_{H+} in the WIPP (~ 9.5), the measured uranium solubility approaches ~ 10^{-7} - 10^{-6} M.

At the same pC_{H+} (~ 9.5), the solubility of uranium was about one order of magnitude higher in GWB than in ERDA-6 (Figure 4-22). This is likely due to the differences in ionic strength and complexant concentration in the two brines (Table 4-4). It is possible that uranium (VI) could undergo some complexation with borate ion near the pC_{H+} value expected in the WIPP (~ 9.5). The borate complexation effect in the WIPP brine was demonstrated on neodymium (III) by Borkowski [2009]. The effect of borate on the uranyl system was confirmed by saturating three ERDA-6 solutions at an initial pC_{H+} of 8.1, 9.6 and 10.5 with sodium tetraborate solid, reaching a total concentration of ~ 5×10^{-2} M tetraborate in solution [Lucchini 2013]. The impact of the tetraborate addition is depicted in Figure 4-22. A significant increase of uranium in solution and a shift of pC_{H+} to values close to the pK_a (9.02) of boric acid at I = 5.0 M, were observed after 55 days of experiments. The change in pC_{H+} can be explained in terms of the strong buffering capacity of the aqueous tetraborate.

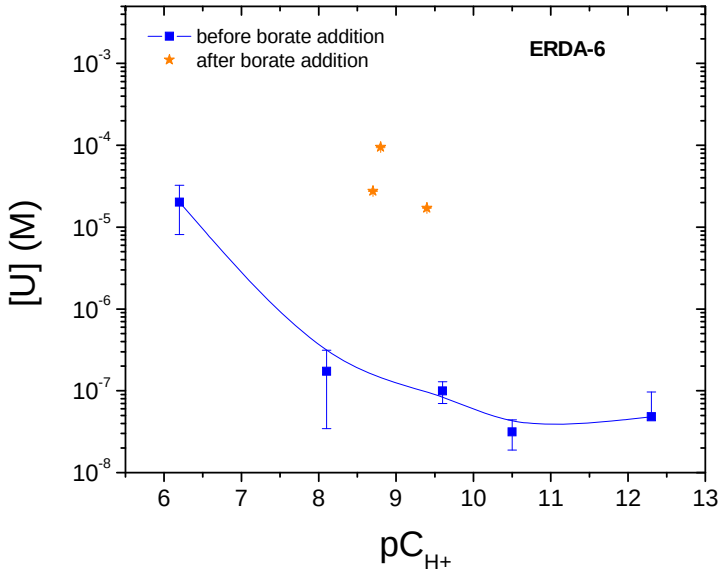

Figure 4-22. Uranium (VI) concentrations versus pC_{H+}, measured in three carbonate-free ERDA-6 brines 55 days after saturation with sodium tetraborate (orange symbols). The blue curve at the bottom of the graph represents the data obtained in ERDA-6 before the addition of tetraborate (polynomial fit) [Lucchini 2013].

At pC_{H+} values up to 10.5, the uranium concentration trends observed over time in carbonate-free ERDA-6 brine (Figure 4-21) indicated that uranium (VI) did not exhibit strongly amphoteric behavior under the conditions investigated.

Our experimental data were compared with the most similar published work, performed by Diaz-Arocas and Grambow [Diaz-Arocas 1998]. They performed uranium (VI) solubility experiments in 5 M NaCl at 25°C and different basic pC_{H+} values, under an argon atmosphere using an over-saturation approach. Their equilibrated uranium concentration data in 5 M NaCl are presented in Table 4-6, along with our WIPP-specific data in ERDA-6, which is the most representative sodium chloride-based WIPP simulated brine (see Table 4-4). The published values were converted from molality to molarity using a density value of 5 M NaCl equal to 1185 g/L. Diaz-Arocas and Grambow reported a uranium solubility of $(2.8 \pm 1.8)\times10^{-5}$ M at $pC_{H+} = 8.9$ in 5 M sodium chloride with a similar experimental approach using argon bubbling to remove carbonate. In contrast, the solubility of uranium in our carbonate-free ERDA-6 brine was $(2.0 \pm 2.0)\times10^{-7}$ M at $pC_{H+} = 8.1$ in ERDA-6 brine (containing 4.31 M NaCl). Our experiments were performed in a nitrogen glovebox with a carbonate-free atmosphere, and the results are more than two orders of magnitude lower than Diaz-Arocas and Grambow's data (Figure 4-21). The lower uranium concentrations reported in our experiments probably reflect the greater extent that carbon dioxide was removed from the brine solutions at the beginning of the experiments, along with a better control of the carbon dioxide-free environment throughout our experiment.

Table 4-6. Uranium (VI) solubility in chloride-based brines (I~5 M) at 25°C and different basic pC_{H+} values, under controlled atmosphere (Ar or N_2) using over-saturation approach. Data from published work [Diaz-Arocas 1998] and [Yamazaki 1992], and these experiments.

Medium	pC_{H+}	Atmosphere	Equ. [U] (M)	Reference
5 M NaCl	6.5	Ar	$(2.8\pm0.9)\times10^{-3}$	[Diaz-Arocas 1998]
5 M NaCl	7.1	Ar	$(4.2\pm1.9)\times10^{-4}$	[Diaz-Arocas 1998]
5 M NaCl	7.6	Ar	$(8.2\pm4.6)\times10^{-5}$	[Diaz-Arocas 1998]
5 M NaCl	8.9	Ar	$(2.8\pm1.8)\times10^{-5}$	[Diaz-Arocas 1998]
Brine	8.4	Air	$(1.80\pm0.05)\times10^{-3}$	[Yamazaki 1992]
Brine	10.4	N_2	$(3.8\pm0.4)\times10^{-7}$	[Yamazaki 1992]
ERDA-6	8.1	N_2	$(1.7\pm1.4)\times10^{-7}$	This work
ERDA-6	9.6	N_2	$(9.9\pm3.0)\times10^{-8}$	This work
ERDA-6	10.5	N_2	$(3.1\pm1.3)\times10^{-8}$	This work

Our data are less comparable to the experimental data obtained by Yamazaki in brine with a nitrogen cover gas [Yamazaki 1992]. At $pC_{H+} = 10.4$, he measured a U(VI) solubility of $(3.8 \pm 0.4)\times10^{-7}$ M, which is ten times higher than our experimental value in ERDA-6 at about the same pC_{H+} (Table 4-6).

4.5 Solubility of Uranium (VI) Solids in Carbonate-free Brines

The uranium (VI) solubility experiments conducted in carbonate-free ERDA-6 and GWB brines using the under-saturation approach (see section 4.3.3) were performed to achieve two goals: (1) to confirm the data obtained in Subtask 1 on the uranium (VI) solubility in carbonate-free brines at different pC_{H+} values, and (2) to investigate the solubility of various uranium solid phases under those experimental conditions. The first part of these goals was developed in section 4.4. In this section, a discussion of the solubilities of the solid uranium phases used is provided.

The solubility of four different uranium (VI) solids is presented in carbonate-free GWB (see section 4.5.1) and ERDA-6 (see section 4.5.2). The results presented herein are for the final measured pC_{H+}, unless otherwise noted in the text.

4.5.1 Solubility of uranium (VI) solids in carbonate-free GWB brine

Figure 4-23 shows the solubility of the four investigated uranium solids in carbonate-free GWB brine as a function of pC_{H+}.

Two distinct pC_{H+} regions could be noted in Figure 4-23. At $pC_{H+} \leq 7.4$, solubilities differed. The uranium peroxide was more soluble, and the uranium precipitates were the least soluble. At $pC_{H+} = 6.3$, the uranium solubility was about 4.5×10^{-5} M for the uranium peroxide, and about 1.8×10^{-6} M for the uranium precipitates. The other two uranium solids (trioxide and hydroxide) had a solubility of about 8.0×10^{-6} M at $pC_{H+} = 6.3$.

At $pC_{H+} \geq 7.4$, however, the four investigated uranium solids had similar solubility in carbonate-free GWB. At $pC_{H+} = 8.2$, the uranium solubility for uranium trioxide, hydroxide, and precipitates was between 5×10^{-6} M and 7×10^{-6} M, while it was slightly higher for the uranium peroxide (10^{-5} M). At $pC_{H+} = 9.3$, the uranium solubility for uranium trioxide, hydroxide and precipitates was about 7×10^{-7} M, and again slightly higher for the uranium peroxide (1.2×10^{-6} M). At $pC_{H+} \geq 7.4$, the uranium precipitates generated in the over-saturation experiments were as soluble as the other uranium solid phases.

Also, as previously described in section 4.3.2.1, the concentration of uranium released in carbonate-free GWB brine was lower at $pC_{H+} = 9.3$ than at any other pC_{H+} values, regardless of the uranium solid phase that was placed in solution. These uranium concentrations measured in solution were about or below 10^{-6} M.

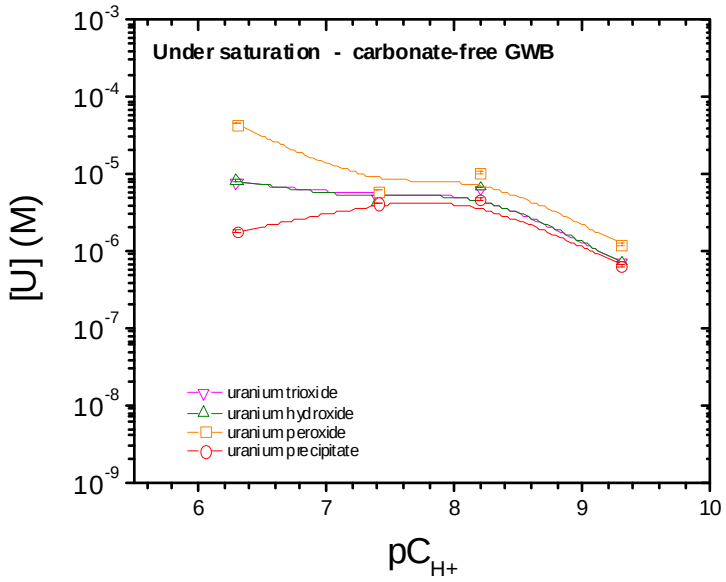

Figure 4-23. Solubility of four uranium solids in carbonate-free GWB solutions in nitrogen controlled atmosphere and at different pC_{H+} values. From the top to the bottom of the legend, the uranium solids are respectively the uranium trioxide, the uranium hydroxide, the uranium peroxide, and a uranium precipitate obtained in over-saturation experiments (polynomial fit).

4.5.2 Solubility of uranium (VI) solids in carbonate-free ERDA-6 brine

In Figure 4-24, the solubility of the four investigated uranium solids in carbonate-free ERDA-6 brine is plotted as a function of pC_{H+}.

Unlike the results obtained in GWB brine (see section 4.5.1), the uranium solubilities obtained in carbonate-free ERDA-6 brine were very different among the four uranium (VI) solid phases investigated.

Over the broad range of pC_{H+} of this study (i.e., from 7 to 12.5), uranium peroxide released the most uranium in ERDA-6 solution. The maximum concentration measured in solution from the dissolution of uranium peroxide was 1.5×10^{-5} M at $pC_{H+} = 9.6$. The uranium release from uranium peroxide was lower at pC_{H+} values other than 9.6 (1.4×10^{-6} M at $pC_{H+} < 9.6$, 3.8×10^{-6} M at $pC_{H+} = 10.5$, 5.2×10^{-6} M at $pC_{H+} = 12.5$). Both uranium peroxide and uranium trioxide appear to have the same solubility at $pC_{H+} = 9.6$ (i.e., 1.5×10^{-5} M). Uranium trioxide solubility is maybe more enhanced at $pC_{H+} = 9.6$, but it decreased with increasing pC_{H+}. The concentration of uranium measured in solution from the dissolution of uranium trioxide was 1.2×10^{-6} M at $pC_{H+} = 7$, 2.5×10^{-7} M at $pC_{H+} = 8.2$ and 1.8×10^{-7} M at $pC_{H+} = 10.5$.

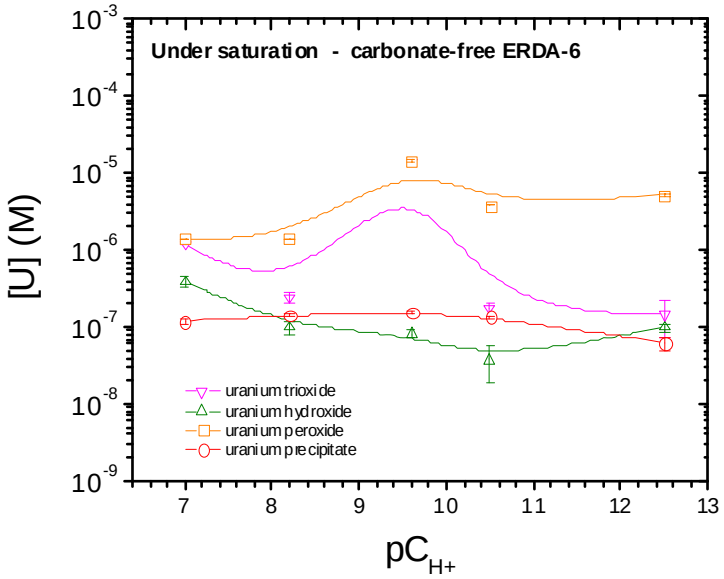

Figure 4-24. Solubility of four uranium solids in carbonate-free ERDA-6 solutions in nitrogen controlled atmosphere and at different pC_{H+} values. From the top to the bottom of the legend, the uranium solids are respectively the uranium trioxide, the uranium hydroxide, the uranium peroxide, and a uranium precipitate obtained in over-saturation experiments (polynomial fit).

The profile of the solubility of uranium hydroxide versus pC_{H+} matched the profile of the solubility of uranium precipitates at $pC_{H+} > 8$. At $pC_{H+} = 8.2$, the uranium solubility for uranium hydroxide was about 10^{-7} M, and the solubility of the uranium precipitates was 1.4×10^{-7} M. At $pC_{H+} = 12.5$, the uranium solubility for uranium hydroxide was 9.8×10^{-8} M, and the solubility of the uranium precipitates was 6.2×10^{-8} M, which was close to the solubility of uranium trioxide at this pC_{H+} value (7.1×10^{-8} M). Between pC_{H+} 8.2 and 12.5, the solubility of the uranium precipitates was a little higher than the solubility of the uranium hydroxide. For example, at $pC_{H+} = 9.6$, the uranium solubility for uranium hydroxide was 8.1×10^{-8} M, and the solubility of the uranium precipitates was 1.5×10^{-7} M.

At a given pC_{H+} value, the uranium steady-state concentration in the brine solution was lower for the uranium hydroxide and the uranium precipitates, which had been previously generated in over-saturation experiments at the same experimental conditions, than in the presence of the peroxide and trioxide uranium phases. At pC_{H+} values between 8.2 and 10.5, the peroxide and trioxide solids used were out of equilibrium with the brine and led to higher apparent solubility.

4.6 Solubility of U(VI) in the Presence of Carbonate

The experimental data obtained in the experiments performed in Subtask 3 (see section 4.3.3) are presented here as a function of pC_{H+}. Figure 4-25 shows the uranium concentrations measured in GWB and ERDA-6 brines in the absence of carbonate and in the presence of initial carbonate concentrations of 2×10^{-4} M and 2×10^{-3} M.

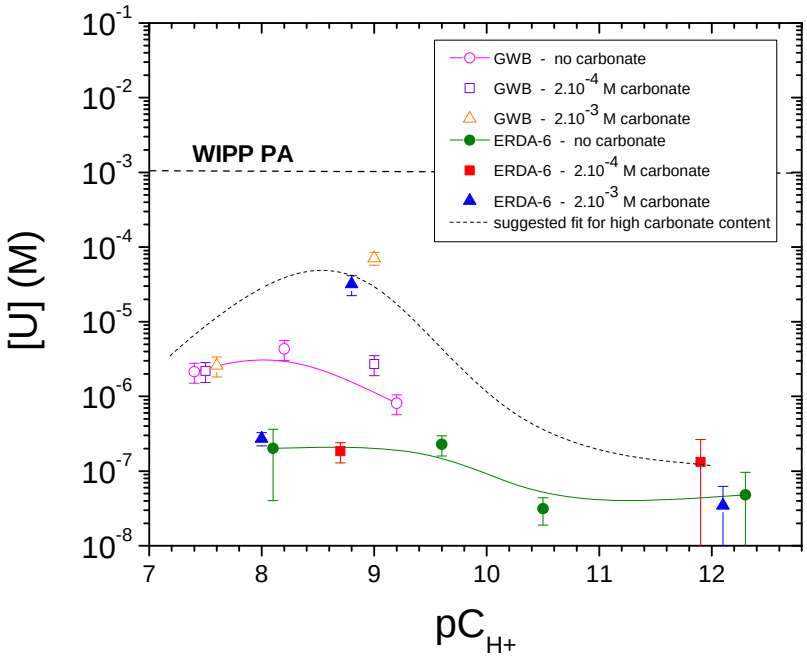

Figure 4-25. Uranium concentrations in ERDA-6 (filled symbols) and GWB (open symbols) versus pC_{H+} in nitrogen controlled atmosphere in the absence or the presence of two concentrations of carbonate (2×10^{-4} M and 2×10^{-3} M) at the beginning of the experiments (polynomial fit). These data correspond to 18 samplings performed over 1073 days. The horizontal dotted line (…...) represents the value of U(VI) solubility considered in the WIPP PA.

It should be noted that the data presented in Figure 4-25 were obtained in solubility experiments using the over-saturation approach, and they may need to be confirmed by experiments using the under-saturation approach. At $pC_{H+} \geq 7$ in GWB brine, steady-state U(VI) concentrations and precipitation were always observed. In ERDA-6 brine, steady-state concentrations were not yet achieved, and the over-saturation experiments have not been

completed at this time. Therefore, the data presented in this report should only be used qualitatively.

Three distinctive regions were noted. The first pC_{H+} region was $7.5 \leq pC_{H+} \leq 8$. In this pC_{H+} region, the uranium concentration was stable in both brines, and was independent of the carbonate concentration. At $pC_{H+} \sim 7.5$ in GWB, the uranium concentrations measured in solution were 1.8×10^{-6} M in the absence of carbonate, 1.6×10^{-6} M in the presence of 2×10^{-4} M carbonate at the beginning of the experiments, and 1.7×10^{-6} M in the presence of 2×10^{-3} M carbonate at the beginning of the experiments. At $pC_{H+} \sim 8$ in ERDA-6, the uranium measured in solution was about 1.3×10^{-7} M, regardless of the presence of high, low, and no carbonate. We do not have a definitive explanation for this because we did not analyze for carbonate throughout the experiment. There are likely multiple contributions to this observation including loss of carbonate at low pC_{H+} (i.e., $CO_{2\,(aq)}$ is expected to be the predominant carbon species in that range of pC_{H+}), precipitation of carbonate phases, and the relatively weak complexation of uranyl with bicarbonate that predominates at these lower pC_{H+} values.

However, there were differences in the uranium solubility due to differences in the composition of the brine: $\sim 10^{-6}$ M in GWB, and $\sim 10^{-7}$ M in ERDA-6. These data indicated that while there was no impact of carbonate in this pC_{H+} region ($7 \leq pC_{H+} \leq 8.5$), there was an observable solubility enhancement due to one or more component of GWB compared to ERDA-6. Based on our investigation of neodymium solubility [Borkowski 2009], we postulated that borate may also play a role in defining the uranium (VI) solubility in this pC_{H+} region. This possibility was confirmed experimentally in section 4.4 and elsewhere [Lucchini 2013]).

The second pC_{H+} region of interest, $8 \leq pC_{H+} \leq 10$, is directly relevant to the WIPP. In this pC_{H+} region, not only there was a compositional effect between the two brines studied (i.e., higher uranium concentrations in GWB than in ERDA-6 for identical carbonate content), but there was also an impact of carbonate on the observed uranium solubility in each brine. At $pC_{H+} \sim 9$, the small effect of borate complexation was still noticeable, since there was still a difference in the uranium concentrations measured in the two brines. However, at $pC_{H+} \sim 9$, the uranium concentrations measured in the presence of the high carbonate concentration were increased by approximately two orders of magnitude, compared to the values at $pC_{H+} \sim 8$, to 1.6×10^{-5} M in ERDA-6, and to about 10^{-4} M in GWB. This could be directly attributed to carbonate complexation at the higher initial carbonate concentrations investigated, since the level of carbonate species (2×10^{-3} M initially) was then in excess to the amounts of uranium introduced in solution. The low carbonate content data (2×10^{-4} M initially) did not reflect as strong of an influence of carbonate on uranium solubility, since these data were similar to the ones obtained in carbonate-free systems.

Lastly, the third pC_{H+} region of interest is at $10 \leq pC_{H+}$. In that pC_{H+} region, beyond the chemical stability range of ERDA-6, the impact of carbonate on the uranium concentration measured in solution could not be observed through the experimental results (see Figure 4-25). The uranium concentrations measured in ERDA-6 were 6.4×10^{-8} M at $pC_{H+} \sim 12.4$ in the absence of carbonate, 1.5×10^{-8} M at $pC_{H+} \sim 11.9$ in the presence of a low amount of carbonate at the beginning of the experiments, and 3.3×10^{-8} M at $pC_{H+} \sim 12.1$ in the presence of a high amount of carbonate at the beginning of the experiments. Hydrolysis is

certainly the predominant pathway in the mechanism of uranium solubility in ERDA-6 at $pC_{H+} \sim 12$.

Our experimental results were in good agreement with the understanding of the effects of carbonate complexation on uranium (VI) solubility in similar media [Clark 1995]. Carbonate can have a significant impact in uranium solubility in a certain range of pC_{H+}, and the extent of this impact is dependent on the amount of carbonate that was introduced in the solution. This conclusion from our experimental work corroborates the observation by Clark [1995] that carbonate complexation will dominate the speciation of the uranyl ion as long as there is ample carbonate-bicarbonate available (see section 3.3). Also, according to Clark, when the uranyl ion concentration exceeds the carbonate concentration, hydrolysis competes with carbonate complexation and plays an increasingly important role [Clark 1995]. This was corroborated by our experimental results for pC_{H+} beyond 9.5.

The range of pC_{H+} when uranium and carbonate generated a complex that was stable in the WIPP simulated brines was determined to be between 8.5 and 9.5. In our WIPP simulated brines, at a pC_{H+} range between 8.5 and 9.5, an effect of carbonate on uranium concentrations was detected when the concentration of carbonate introduced initially into the solutions was 2×10^{-3} M. The initial carbonate concentration of 2×10^{-3} M was about an order of magnitude higher than the concentration of uranium introduced in solution when precipitation occurred in our experiments. This excess of carbonate could have allowed the soluble 2:3 complex, $UO_2(CO_3)_3^{4-}$, or other polynuclear complexes suggested by Grenthe *et al*. and Clark [Grenthe 1994, Clark 1995] to form in our experimental solutions (see section 3.3). Future spectroscopy work on our experimental samples could help to identify the major uranium carbonate species in solution.

Our experimental results, though, were different from the data collected for carbonate effects on uranium (VI) solubility in similar media, and published in the literature [Grenthe 1984, Kramer-Schnabel 1992, Yamazaki 1992, Reed 1997, Peper 2004]. For example, the experimental curves of the solubility of UO_2CO_3 obtained by Kramer-Schnabel *et al*. and Grenthe *et al*. (Figure 3-3) established the uranium concentration in solution at the millimole level or higher when the concentration of carbonate is higher than micromole level. In our experiments, the uranium concentrations measured in solution at any pC_{H+} and for carbonate concentrations as high as 2mM were below the millimole level. Differences in the experimental conditions between Kramer-Schnabel's and Grenthe's experiments, and our experiments can explain the different results. Kramer-Schnabel *et al.* and Grenthe *et al.* performed their experiments in sealed containers with a CO_2 atmosphere, in the pC_{H+} region 3 to 6, at a relatively low ionic strength ($I \leq 3$ M), and in the presence of a non-complexant medium, sodium perchlorate. Our experiments were performed using an initial amount of carbonate, at $pC_{H+} > 7$, in high ionic strength solutions ($I > 4$ M) in the presence of cations that can precipitate carbonate (Mg^{2+}, Ca^{2+}). Therefore, slight losses of carbonate by complexation with Mg^{2+} and Ca^{2+}, and/or as the loss of gas-phase CO_2 during sampling events, could account for the discrepancies observed on the impact of carbonate concentration on uranium solubility between the present work and those in the literature.

Yamazaki *et al.* reported millimole concentrations of uranium (Figure 3-2) in his U(VI) solubility experiments performed in a synthetic brine at $pC_{H+} = 8.4$ and in an air

atmosphere [Yamazaki 1992]. Yamazaki's results at that pC_{H+} value were over-estimated, by an order of magnitude, the results we obtained at even the highest carbonate concentration introduced in the solutions ($[CO_3^{2-}]_{total} = 2\times10^{-3}$ M). The highest uranium concentration we measured in our experiments was 7.4×10^{-5} M in GWB, at $pC_{H+} \sim 9$ and in the presence of 2mM. The difference between Yamazaki's results and ours is not readily explained based on what is published, although one speculative explanation is that there was more carbonate present in this system than acknowledged by the author. At $pC_{H+} = 10.4$, however, in a brine solution with an initial concentration of bicarbonate of 0.11 mM, Yamazaki *et al.* measured uranium concentrations in solution about 3.5×10^{-7} M. These uranium concentrations were approximately the same order of magnitude that we obtained in our experiments at the same pC_{H+} and CO_3^{2-} conditions (Figure 4-36). At $pC_{H+} = 10.4$, we expect hydrolysis to predominate over carbonate complexation. These data were a few orders of magnitude lower than the data obtained by Reed [1997]. Reed's experiments were conducted under a hydrogen atmosphere at 25±5°C, and the uranium (VI) concentration was stable at approximately 1×10^{-4} M when measured as a function of time in ERDA-6 brine at $pC_{H+}\sim10$ in the presence of ~up to 10 mM CO_3^{2-} initially placed in solution [Reed 1997]. The amount of carbonate placed in solution in Reed's work was 5 times greater than in our experiments, and the vessels were completely sealed during the experiments, so possible loss of carbonate was unlikely. The amount of uranium initially introduced in solution (10^{-4} M) in Reed's experiments was 12 times smaller than in our experiments. Consequently, the carbonate/uranium ratio was greater in Reed's experiments than in our experiments. Therefore, a greater uranium solubility in the presence of carbonate was expected, and indeed measured in Reed's experiments.

5.0 CONCLUSION

The solubility of uranium (VI) was determined in WIPP-relevant brines as a function of pC_{H+} and ionic strength, both in the absence and presence of carbonate. Additionally, a literature review on the solubility of uranium (VI) under WIPP-related conditions was conducted.

The solubility data for uranium (VI) in WIPP brine presented in this report accomplished the following:

- Provided the first WIPP-relevant data for the VI actinide oxidation state that established the solubility of uranium (VI) over an extended pC_{H+} range for GWB and ERDA-6 brines in the absence or presence of carbonate.
- Established an upper limit of ~ 10^{-6} M uranyl concentration at the reference pC_{H+} WIPP case in the absence of carbonate, and an upper limit of ~ 10^{-4} M uranyl concentration at the reference pC_{H+} WIPP case (i.e., pC_{H+} ~ 9.5) in the presence of 2mM carbonate.
- Demonstrated that high pC_{H+} values lead to low uranium solubility due to hydrolysis, in carbonate-free and low carbonate content WIPP brines. At $pC_{H+} \geq 10.5$, hydrolysis overwhelms carbonate effects. No amphoteric effect was observed in WIPP simulated brines at high pC_{H+} values.
- Demonstrated a small effect of borate complexation in the pC_{H+} range [7.5 – 10].

The observed effects of carbonate on the solubility of U(VI) in WIPP-specific brines are the most relevant to the current PA assumption that the solubility of U(VI) will be 1 mM or less. These experimental data were the first data on the impact of carbonate on uranium solubility in WIPP brines. For WIPP-related conditions (i.e., pC_{H+} ~ 9.5), the highest uranium solubility measured was ~ 10^{-4} M, which was an order of magnitude lower than the uranium (VI) solubility currently assumed by WIPP PA. This high uranium solubility was obtained at a carbonate concentration (2×10^{-3} M), which was ~ 10 times higher amount of carbonate expected in the WIPP due to the buffering of the MgO barrier material.

The data we reported in this document showed that the 1 mM value for uranium (VI) solubility used in WIPP PA was conservative, by over a factor of 50, relative to our experimental results. Our data clearly support the current position on An(VI) solubility under WIPP-relevant conditions.

6.0 QUALITY ASSURANCE, DATA TRACEABILITY AND DOCUMENTATION

The data presented in this report were generated in compliance with the QAPD. The research was performed as a part of Task 1 of the Test Plan entitled "Solubility/Stability of Uranium (VI) in WIPP Brines" and designated LCO-ACP-02. The documentation for the experiments performed is found in four Test Plan-specific scientific notebooks designated ACP-TIP-002/1, ACP-TIP-002/3, ACP-TIP-002/4 and ACP-TIP-002/5 and in a series of 47 data packages designated U0 to U37, and U65 to U74. Table 6-1 gives the title of these 47 data packages. Copies of the scientific notebooks and the data packages are kept at the LANL-CO Record Center. Data shown in ACRSP-generated figures in this document are traceable to the scientific notebooks and data packages. Documentation of this linkage is included in data package U74. Any other figures included in this report are based on literature data, and the associated references are mentioned in the caption of the figures.

Table 6-1. Titles of the data packages U0 to U37, and U65 to U74 associated with this document.

Data package	Title
U0	LCO-ACP-02 Task 1 –Subtask 1 – U0 – U stock
U1	LCO-ACP-02 Task 1 – Subtask 1 – U1 – Sampling #1
U2	LCO-ACP-02 Task 1 – Subtask 1 – U2 – Sampling #2
U3	LCO-ACP-02 Task 1 – Subtask 1 – U3 – Sampling #3
U4	LCO-ACP-02 Task 1 – Subtask 1 – U4 – Sampling #4
U5	LCO-ACP-02 Task 1 – Subtask 1 – U5 – Sampling #5
U6	LCO-ACP-02 Task 1 – Subtask 1 – U6 – Sampling #6
U7	LCO-ACP-02 Task 1 – Subtask 1 – U7 – Sampling #7
U8	LCO-ACP-02 Task 1 – Subtask 1 – U8 – Sampling #8
U9	LCO-ACP-02 Task 1 – Subtask 1 – U9 – Sampling #9
U10	LCO-ACP-02 Task 1 – Subtask 1 – U10 – Sampling #10
U11	LCO-ACP-02 Task 1 – Subtask 1 – U11 – Sampling #11
U12	LCO-ACP-02 Task 1 – Subtask 1 – U12 – Sampling #12
U13	LCO-ACP-02 Task 1 – Subtask 1 – U13 – Sampling #13
U14	LCO-ACP-02 Task 1 – Subtask 1 – U14 – Sampling #14
U15	LCO-ACP-02 Task 1 – Subtask 1 – U15 – Sampling #15
U16	LCO-ACP-02 Task 1 – Subtask 1 – U16 – Sampling #16
U17	LCO-ACP-02 Task 1 – Subtask 1 – U17 – Sampling #17
U18	LCO-ACP-02 Task 1 – Subtask 1 – U18 – Sampling #18
U19	LCO-ACP-02 Task 1 – Subtask 1 – U19 – Sampling #19
U20	LCO-ACP-02 Task 1 – Subtask 3 – U20 – Sampling #1
U21	LCO-ACP-02 Task 1 – Subtask 3 – U21 – Sampling #2
U22	LCO-ACP-02 Task 1 – Subtask 3 – U22 – Sampling #3
U23	LCO-ACP-02 Task 1 – Subtask 3 – U23 – Sampling #4
U24	LCO-ACP-02 Task 1 – Subtask 3 – U24 – Sampling #5

U25	LCO-ACP-02 Task 1 – Subtask 3 – U25 – Sampling #6
U26	LCO-ACP-02 Task 1 – Subtask 3 – U26 – Sampling #7
U27	LCO-ACP-02 Task 1 – Subtask 3 – U27 – Sampling #8
U28	LCO-ACP-02 Task 1 – Subtask 3 – U28 – Sampling #9
U29	LCO-ACP-02 Task 1 – Subtask 3 – U29 – Sampling #10
U30	LCO-ACP-02 Task 1 – Subtask 3 – U30 – Sampling #11
U31	LCO-ACP-02 Task 1 – Subtask 3 – U31 – Sampling #12
U32	LCO-ACP-02 Task 1 – Subtask 3 – U32 – Sampling #13
U33	LCO-ACP-02 Task 1 – Subtask 3 – U33 – Sampling #14
U34	LCO-ACP-02 Task 1 – Subtask 3 – U34 – Sampling #15
U35	LCO-ACP-02 Task 1 – Subtask 3 – U35 – Sampling #16
U36	LCO-ACP-02 Task 1 – Subtask 3 – U36 – Sampling #17
U37	LCO-ACP-02 Task 1 – Subtask 3 – U37 – Sampling #18
U65	LCO-ACP-02 Task 1 – Subtask 8 – U65 – Sampling #1
U66	LCO-ACP-02 Task 1 – Subtask 8 – U66 – Sampling #2
U67	LCO-ACP-02 Task 1 – Subtask 8 – U67 – Sampling #3
U68	LCO-ACP-02 Task 1 – Subtask 8 – U68 – Sampling #4
U69	LCO-ACP-02 Task 1 – Subtask 8 – U69 – Sampling #5
U70	LCO-ACP-02 Task 1 – Subtask 8 – U70 – Sampling #6
U71	LCO-ACP-02 Task 1 – Subtask 8 – U71 – Sampling #7
U72	LCO-ACP-02 Task 1 – Subtask 8 – U72 – Sampling #8
U73	LCO-ACP-02 Task 1 – Subtask 8 – U73 – Sampling #9
U74	Summary Data Package for this document

7.0 REFERENCES

[Åberg 1970] Åberg M., Structure of the predominant hydrolysis products of uranyl (VI) in solution, Acta Chemica Scandinavica, **24** (1970) 2901-2915.

[Borkowski 2009] Borkowski M., J.F. Lucchini, Reed D.T., M.K. Richmann, Actinide (III) Solubility in WIPP Brine: Data Summary and Recommendations, LCO-ACP-08, LANL-CO\ACRSP Report. LA-14360, Los Alamos, NM: Los Alamos National Laboratory (2009).

[Brady 1948] Brady L.J., C.D. Susano, C.E. Larson, Chemical and Physical Properties of Uranium Peroxide, United States Atomic Energy Commission, Oak Ridge, AECD-2369 Report (1948).

[Brush 1990] Brush L.H., Test Plan for Laboratory and Modeling Studies of Repository and Radionuclide Chemistry for the Waste Isolation Pilot Plant, Report SAND90-0266, Sandia National Laboratories. Albuquerque, NM. (1990).

[Brush 2003] Brush L.H., Y. Xiong, Calculation of Actinide Solubilities for the WIPP Compliance Recertification Application, Sandia National Laboratories Carlsbad Programs Group, Carlsbad, NM, May 8, 2003, ERMS 529131.

[Brush 2009] Brush L.H., Y. Xiong, J.J. Long, Results of the Calculations of Actinide Solubilities for the WIPP CRA-2009 PABC, Sandia National Laboratories Carlsbad Programs Group, Carlsbad, NM, Analysis Report, October 7, 2009. ERMS 552201.

[Cahill 1990] Cahill, A.E.,L.E. Burkhart, Continuous precipitation of uranium with hydrogen peroxide, Metallurgical Transactions B 2,**1B** (1990) 819.

[Choppin 2003] Choppin G.R., Actinide Speciation in the Environment, Radiochimica Acta, **91** (2003) 645.

[Clark 1995] Clark D.L., D.E Hobart., and M.P.Neu, Actinide Carbonate Complexes and their Importance in Actinide Environmental Chemistry, Chemical Reviews, **95** (1995) 25.

[Diaz-Arocas 1998] Diaz Arocas P., B.Grambow, Solid-liquid Phase Equilibria of U(VI) in NaCl Solutions, Geochimica et Cosmochimica Acta, **62/2** (1998) 245.

[DOE 1996] Title 40 CFR Part 191 Compliance Certification Application for the Waste Isolation Pilot Plant, DOE/CAO-1996-2184, October 1996, DOE Carlsbad Field Office, Carlsbad, NM.

[EPA 2005] Performance Assessment Issues. Letter from E. Cotsworth, U.S. Environmental Protection Agency Office of Radiation and Indoor Air, Washington DC, to Ines Triay, U.S. Department of Energy Carlsbad Field Office, March 4, 2005.

[EPA 2010] Evaluation of the Compliance Recertification Actinide Source Term, Backfill Efficacy and Culebra Dolomite Distribution Coefficient Values, Technical Support Document for Section 194.24, November 2010, U.S. Environmental Protection Agency Office of Radiation and Indoor Air.

[Fanghänel 2002] Fanghänel, T.; Neck, V.: Aquatic Chemistry and Solubility Phenomena of Actinide Oxides/Hydroxides. Pure and Applied Chemistry **74/10** (2002) 1895.

[Grenthe 1984] Grenthe, I., D. Ferri, F. Salvatore, and G. Riccio., Studies on Metal Carbonate Equilibria. Part 10. A Solubility Study of the Complex Formation in the Uranium (VI)-Water-Carbon Dioxide (g) System at 25º. Journal of Chemical Society, Dalton Trans. (1984) 2439.

[Guillaumont 2003] Guillaumont R., T. Fanghanel, J. Fuger, I. Grenthe, V. Neck, D.A. Palmer, and M. H. Rand, Update on the Chemical Thermodynamics of Uranium, Neptunium, Plutonium, Americium and Technetium, ed., Mompean, F.I., Illemassene, M., Domenech-Orti, C., Ben Said, K., Nuclear Energy Agency, Organization for Economic Co-operation and Development, vol. **5**, *Chemical Thermodynamics*, North Holland Elsevier Science Publishers B. V., Amsterdam, The Netherlands (2003).

[Hobart 1996] Hobart D.E., R.C. Moore, Analysis of Uranium (VI) Solubility Data for WIPP Performance Assessment, Sandia National Laboratories, unpublished report, May 28, 1996. Albuquerque, NM.

[Katz 1986] Katz J.J., G.T. Seaborg, and L.R. Morss, The Chemistry of the Actinide Elements., 2nd eds., New York, NY: Chapman and Hall. Vols. **1-2** (1986).

[Kramer-Schnabel 1992] Kramer-Schnabel U., H. Bischoff, R.H. Xi, and G. Marx, Solubility products and complex formation equilibria in the systems uranyl hydroxide and uranyl carbonate at 25°C and I=0.1M, Radiochimica Acta **56** (1992) 1838.

[Lin 1998] Lin M.R., P. Paviet-Hartmann, Y. Xu, and W.H. Runde, Uranyl Compounds in NaCl Solutions,: Structure, Solubility and Thermodynamics, American Chemical Society, Division of Environmental Chemistry, Preprints of Extended Abstracts. 216th ACS National Meeting, Boston Massachusetts, August 23-27, 1998, 38:208

[Lucchini 2007] Lucchini J-F, M. Borkowski, M.K. Richmann, S. Ballard, and D.T. Reed, Solubility of Nd^{3+} and UO_2^{2+} in WIPP brine as oxidation-state invariant Analogs for Plutonium, Journal of Alloys and Compounds, **444-445** (2007) 506.

[Lucchini 2010a] Lucchini J.F., H. Khaing, M. Borkowski, M.K. Richmann, D.T. Reed, Actinide (VI) Solubility in Carbonate-free WIPP Brine: Data Summary and Recommendations, LCO-ACP-10, LANL-CO\ACRSP Report. LA-UR-10-00497. Los Alamos, NM: Los Alamos National Laboratory (2010).

[Lucchini 2010b] Lucchini J.F., H. Khaing, D.T. Reed, Uranium (VI) Solubility in Carbonate-free ERDA-6 Brine, Scientific Basis for Nuclear Waste Management XXXIV, edited by K.L. Smith, S. Kroeker, B. Uberuaga, K.R. Whittle, Material Research Society Symposium Proceedings, Volume 1265. LA-UR-10-01817 (2010).

[Lucchini 2013] Lucchini J.F., M. Borkowski, M.K. Richmann, D.T. Reed, Uranium (VI) Solubility in Carbonate-free WIPP Brine, Radiochimica Acta, **101**(2013) 391.

[Morss 2006] Morss L.R., N. Edelstein, and J. Fuger, The Chemistry of the Actinide and Transactinide Elements, 3rd Ed., Springer, Volume **4** (2006).

[Moulin 2001] Moulin V., C. Moulin, Radionuclide Speciation in the Environment: a Review, Radiochimica Acta, **89** (2001) 773.

[Nitsche 1992] Nitsche H., A. Muller, E.M. Standifer, R.S. Deinhammer, K. Becraft, T. Prussin, and R.C. Gatti, Dependence of Actinide Solubility and Speciation on Carbonate Concentration and Ionic-Strength in Groundwater, Radiochimica Acta **58/59** (1992) 27.

[Novak 1996] Novak C.F., R.C. Moore, Estimates of Dissolved Concentrations for III, IV, V, and VI Actinides in Salado and Castile Brine Under Anticipated Repository Conditions, Sandia National Laboratories Technical Memorandum, March 28, 1996.

[Palmer 1995] Palmer D.A., C. Nguyen-Trung, Aqueous Uranyl Complexes. 3. Potentiometric Measurements of the Hydrolysis of Uranyl (VI) Ion at 25ºC, Journal of Solution Chemistry, Vol. **24**, No.**12** (1995) 1281.

[Palmer 1996] Palmer C.E., Private Communication to R. Van Bynum (SAIC/SNL) from C. Palmer (LLNL), dated February 27, 1996, reported by Hobart and Moore (1996).

[Peper 2004] Peper S.M., L.F. Brodnax, S.E. Field, R.A. Zehnder, S.N. Valdez, W.H. Runde, Kinetic Study of the Oxidative Dissolution of UO_2 in Aqueous Carbonate Media, Ind. Eng. Chem. Res. **43** (2004) 8188.

[Rai 1995] Rai D., A.R. Felmy, S.P. Juracich, and L.F.Rao, Estimating the Hydrogen Ion Concentration in Concentrated NaCl and Na_2SO_4 electrolytes, Report SAND94-1949, Sandia National Laboratories, Albuquerque, NM. 1995.

[Reed 1997] Reed, D.T., D. G. Wygmans, Actinide Stability/Solubility in Simulated WIPP Brine, WPO44625. Argonne, IL: Argonne National Laboratory, Actinide Speciation and Chemistry Group, Chemical Technology Group (1997).

[Runde 2000] Runde W. The Chemical Interactions of Actinides in the Environment. Los Alamos Science, **26** (2000) 330.

[SOTERM 2009] Title 40 CFR Part 191 Subparts B and C Compliance Recertification Application 2009, Appendix PA, Attachment SOTERM, DOE Carlsbad Field Office, Carlsbad, NM.

[TWBIR-2004] U.S. Departement of Energy (DOE), Transuranic Waste Baseline Inventory Report – 2004, Revision 0, DOE/TRU-2006-3344, DOE Carlsbad Field Office, Carlsbad, NM (2006).

[Van Soest 2012] Van Soest, G. Performance Assessment Inventory Report – 2012, PAIR 2012. INV-PA-08, LANL-CO\Inventory Report, Los Alamos, NM: Los Alamos National Laboratory (2012).

[Yamamura 1998] Yamamura, T., A. Kitamura, A. Fukui, S. Nishikawa, T. Yamamoto., and H. Moriyama, Solubility of U(VI) in highly basic solutions, Radiochimica Acta **83** (1998) 139.

[Yamazaki 1992] Yamazaki H., B. Lagerman, V. Symeopoulos, and G.R. Choppin, Solubility of Uranyl in Brine, Radioactive Waste Management, **1992** (1992) 1607.